Review | Received 5 July 2024; Accepted 25 August 2024; Published 9 September 2024
https://doi.org/10.55092/rse20240009

Progress in constructing stable dendrite-free sodium metal anode via artificial electrolyte-electrode interface layer

Xiaowei Zhu, Wenwu Mo, Huanyu Li, Shaojie Hu and Lijuan Zhang*

Beijing Key Laboratory for Green Catalysis and Separation, Centre of Excellence for Environmental Safety and Biological Effects, College of Chemistry and Life Science, Beijing University of Technology, Beijing 100124, China

* Correspondence author; E-mail: zhanglj1997@bjut.edu.cn.

Abstract: With the advantages of high theoretical specific capacity (1166 mAh g^{-1}) and low redox potential (–2.71 V), as well as be abundant in resources and low in cost, metallic Na is expected to be used as a promising candidate for the anode material in next-generation high performance secondary batteries. However, factors such as the unstable solid electrolyte interface, unpredictable dendritic growth, and substantial volume change during plating/stripping have hampered the development of sodium metal anodes. A reasonably designed artificial interfacial layer can better stabilize the sodium metal anode, which has been extensively investigated by researchers. This paper reviews the recent advances in the protection of sodium metal anodes by constructing different types of artificial interfacial layers, including inorganic, organic, and hybrid interface layers. Additionally, it discusses the issues and underlying causes associated with sodium metal anodes, and offers an outlook on their future development.

Keywords: sodium metal anode; artificial interfacial layer; dendrite growth; secondary battery; interface engineering

1. Introduction

Nowadays, the world is facing the depletion of non-renewable resources and further environmental degradation, which are seriously hindering sustainable development across various fields. Therefore, developing renewable energy sources, as well as efficient energy storage and conversion technologies, is critical for future growth [1,2]. New clean energy sources such as solar energy and wind energy are susceptible to environmental and other factors, do not have good stability. So it is necessary to develop large-scale storage systems to make full use of these clean energy sources [3]. Although lithium batteries currently occupy a dominant position in the field of energy storage, it is urgent to find new substitutes due to the increasing consumption of lithium resources [4–9]. Sodium resources are abundant

in the Earth's crust, and sodium metal anodes have a high theoretical capacity (approximately 1166 mAh g^{-1}) and a low redox potential (–2.71 V compared to the standard hydrogen electrode), making sodium metal batteries a hot topic of research [10,11].

However, there are significant challenges associated with sodium metal anodes. Firstly, due to the high reactivity of sodium metal, a solid electrolyte interphase (SEI) layer forms on its surface during the cycle when it comes into contact with the electrolyte. Because sodium metal anodes undergo significant volume fluctuations during charge and discharge cycles, the SEI layer is prone to cracking, exposing fresh Na to the electrolyte, leading to repeated SEI formation. This repeated breaking and reforming process consumes active material (Na) and electrolyte, resulting in reduced Coulombic efficiency and shortened cycle life. The situation is further exacerbated by the fact that sodium metal anodes exhibit uneven ion flux during deposition, leading to non-uniform sodium ion transport and localized protrusions. The "tip effect" during the growth process intensifies these protrusions, eventually resulting in the formation of dendritic sodium structures. The continued growth of sodium dendrites poses significant safety risks, as they may penetrate the separator and cause internal short circuits within the battery [12,13].

People have attempted to address these issues by making improvements to various battery components, such as current collectors, electrodes, and electrolytes. Using high-surface-area current collectors, such as 3D or porous collectors made from carbon and metals, can significantly reduce local current density [14,15]. However, this approach requires pre-depositing metal on the collector surface, which is cumbersome as it involves repeatedly disassembling the battery. Additionally, during deposition, sodium tends to accumulate on the substrate surface, leading to uncontrollable volume changes and reduced spatial utilization of the current collector [16,17]. Modifying the solvent, salt concentration, and additives in the electrolyte to adjust the morphology and composition of the SEI can also enhance the functionality of sodium metal anodes [18–20]. Nevertheless, it is challenging to precise regulate the composition and uniformity of the SEI layer produced by this approach. Compared to liquid electrolytes, solid-state electrolytes (SSEs) show better prospects due to their higher theoretical energy density and improved safety, but they face challenges such as poor ionic conductivity and high interfacial resistance at solid-solid interfaces [21]. In contrast, constructing artificial interfacial layers on the electrode surface through physical or chemical methods is easier, and the composition of the interfacial layer can be conveniently adjusted to improve electrode performance [22,23]. This method is simple, efficient, and holds good potential for practical applications.

Therefore, this paper reviews the research progress on the design of artificial interfacial layers for sodium metal anodes. It begins by introducing the main challenges associated with sodium metal anodes, including an analysis of the mechanisms behind sodium dendrite formation, the instability of the SEI layer, and the impact of electrode volume changes during cycling. Then, the methods and principles for constructing inorganic, organic, and inorganic-organic composite interfacial layers are discussed sequentially based on the composition of the artificial interfacial layers, with a comparison of their effectiveness. Finally, the

development of artificial interfacial layers is summarized and discussed, aiming to provide meaningful references for the readers.

2. The current dilemma of sodium metal anode

Due to the strong demand for higher battery energy density, alkali metal secondary batteries have reignited research interest [24]. Compared to lithium metal, sodium metal is more reactive, and the naturally formed solid electrolyte interphase (SEI) is less stable and more prone to being pierced by dendrites growing on the metal surface [25]. Additionally, the continuous exposure of the metal surface leads to ongoing electrolyte consumption, eventually causing battery failure. Unlike embedded anodes such as graphite or alloy-type anodes such as silicon, sodium metal anodes, which lack a host structure, experience significant volume fluctuations during plating and stripping. This further damages the naturally fragile SEI layer, resulting in gradually decreasing Coulombic efficiency, very short cycle life, and serious safety risks [26–28].

2.1. Growth of the Na dendrites

The growth process of Na dendrites is shown in Figure 1a. As sodium is deposited, the volume of the sodium metal undergoes significant changes. This volume change causes the naturally non-dense and unstable SEI layer to crack and form fractures. At these fractures, the diffusion barrier for sodium ions is lower, leading to preferential and uneven deposition of sodium [29]. The repeated plating and stripping processes result in noticeable dendritic sodium forming at these cracks, which, once it reaches a certain extent, detaches from the electrode, becoming "dead sodium." Additionally, the fresh sodium exposed to the electrolyte will form more SEI, increasing the porosity of the sodium anode in the long run, depleting the electrolyte and active sodium, and leading to poor cycling stability [30,31].

The dendrite growth of alkali metals is a complex electrochemical process influenced by a number of factors, including current density, overpotential, alkali metal ion concentration, and others. Chazalviel and Rosso *et al*. proposed space charge models based on different systems to explain the growth behaviour of alkali metal dendrites [32,33]. The existence of a concentration gradient of alkali metal ions in the electrolyte is mainly caused by the fact that the deposition and migration rates of the ions differ significantly in the electrolyte [24]. This difference gives rise to a concentration polarization at the interface, resulting in a higher local space charge density, which affects the deposition of alkali metal ions and preferentially deposits them at geometric bumps [34]. Sand's time is employed to clarify the time that causes the formation of alkali metal dendrites, as indicated in the Equation (1) below [35].

$$\tau_{Sand} = \pi D \frac{(C_0 e)^2}{(2Jt_a)^2} \quad (1)$$

Where D, C_0, e, J, t_a are the ion diffusion coefficient, the initial cation concentration, the elementary positive charge, the applied current density, and the number of transfers of conjugated anions, respectively. Within τ_{Sand}, the cation concentration at the electrode

surface is always maintained around zero and an equilibrium is achieved for the embedding and de-embedding energy of metal ions. With time, the excess metal ions will be gradually generated and tend to be reduced and deposited on the electrode surface, causing the growth of dendrites, from which It can be seen that the longer τ_{Sand} is the more favourable to inhibit the growth of dendrites [36,37]. On the other hand, the deposition of Na^+ on an SEI-covered electrode involves three main steps: the desolvation of Na^+, the diffusion of Na^+ on the SEI (which includes both surface and bulk diffusion), and the reaction between electrons transferred from the electrode and Na^+ [38,39]. Compared to the electron transfer at the SEI/electrode interface, the diffusion rate of Na^+ within the SEI layer is the slowest and is the rate-determining step for the deposition morphology [40]. Especially at high current densities, the uneven flow of Na^+ leads to greater polarization and more pronounced Na^+ diffusion rate limitations, causing the deposition direction of Na^+ to be more vertically oriented and making dendrite formation more likely [30]. Hence, the interfacial diffusion barrier of SEI plays a pivotal role in dendrite growth. Furthermore, the mechanical properties of the SEI layer also impact dendrite growth. Filhol *et al.* investigated the dendrite growth mechanism of Li, Na, and Mg using density functional theory (DFT). The comparison revealed that sodium metal exhibits the lowest critical overpotential, rendering it thermodynamically easier to form dendrites compared to lithium and magnesium [41]. The construction of interfacial layers with high mechanical properties can effectively inhibit the growth of dendrites. According to Monroe and Newman, when the shear modulus of the diaphragm in contact with the metal deposit is higher than twice the shear modulus of that deposited metal, the roughness of the deposited surface is lower, which effectively guides the homogeneous deposition of the metal ions [42]. Inspired by the foregoing, the local current density can be reduced by constructing three-dimensional current collectors [43,44], modulation of electrolyte composition [45,46] or construction of an artificial SEI layer [47] to form a high ionic conductivity rate interface on the alkali metal anode surface to enhance uniform deposition of alkali metal ions. All these methods are favourable for prolonging the Sand's time, which in turn reduces the generation of dendrites.

In addition, Na dendrites are not exactly similar to Li dendrites. Figure 1b shows some of the physical and chemical properties of sodium metal and lithium, and these differences lead to the formation of dendrites with different properties [48]. For example, Hong *et al.* compared the mechanical stability of Na dendrites and Li dendrites (Figure 1c). Under the action of mechanical pressure, the morphology of Li dendrites is more complete, while the mechanical stability of Na dendrites is poor, and it is easier to form dead Na [49]. This difference may be due to the weaker chemical bonds between Na dendrites and the SEI layer, along with Na's higher reactivity and lower Young's modulus. Therefore, it is necessary to further investigate the growth mechanisms of sodium dendrites to better improve sodium metal anodes.

2.2. Unstable SEI layer

The concept of the SEI was first introduced by Peled and colleagues. They discovered that when alkali metal anodes come into contact with non-aqueous electrolytes, a passivation layer forms due to the high reactivity of the alkali metal, which blocks electrons while allowing ion conduction [50]. This phenomenon was subsequently explained by Goodenough *et al.* through the frontier molecular orbital theory [51]. The SEI layer is formed when the electrochemical potential at the anode surface falls outside the electrolyte's electrochemical stability window. Specifically, when the electrochemical potential (μ_A) at the anode is higher than the separation energy of the lowest unoccupied molecular orbital (LUMO) of the electrolyte, the electrolyte gains electrons from the anode. The resulting reduction products form the SEI layer, which adheres to the metal surface. Similarly, when the redox potential (μ_C) at the cathode is lower than the highest occupied molecular orbital (HOMO) of the electrolyte, the electrolyte will be oxidised due to the loss of electrons (Figure 1d) [52]. The electrolyte is only thermodynamically stable when both μ_A and μ_C are within the voltage window of the electrolyte. During the initial charging (plating), the μ_A of Na metal is higher than the LUMO of most electrolytes, and the anode spontaneously transfers available electrons to the electrolyte, where solvents, salts, additives, and other components of the electrolyte are reduced on the surface of the sodium metal anode to produce a passivation film known as the SEI layer. In addition, Sodium metal is a highly reactive metal, prone to chemical reactions with many substances, including solutes or solvents in the electrolyte. These reactions form a film on the surface of the sodium metal, which can offer some degree of protection against further reactions. However, the structure, composition, and stability of this film differ from the SEI layer formed during the charging process [24,53].

The SEI composition primarily includes inorganic compounds, organic materials, and polymers [22]. Ideally, an *in-situ* formed SEI coating on the anode surface can isolate the electrode from the electrolyte, preventing further reactions between them [54]. Additionally, due to the ion conductivity and electrical insulation properties of the SEI layer, it is designed to enhance the safety and cycling performance of the battery. Unfortunately, naturally formed SEI layers have poor deformation resistance, and the volume fluctuations of sodium during battery cycling can lead to SEI layer cracking [55]. These cracks result in uneven deposition of Na^+, leading to the growth of dendrites, which, once they reach a certain size, detach and form "dead" sodium. On the other hand, continuous reactions between the electrolyte and the sodium metal on the anode surface cause the formation of new SEI layers, reducing the cycling efficiency of the battery [56,57]. Therefore, creating a dense artificial interfacial layer with specific mechanical strength is crucial for stabilizing sodium metal anodes.

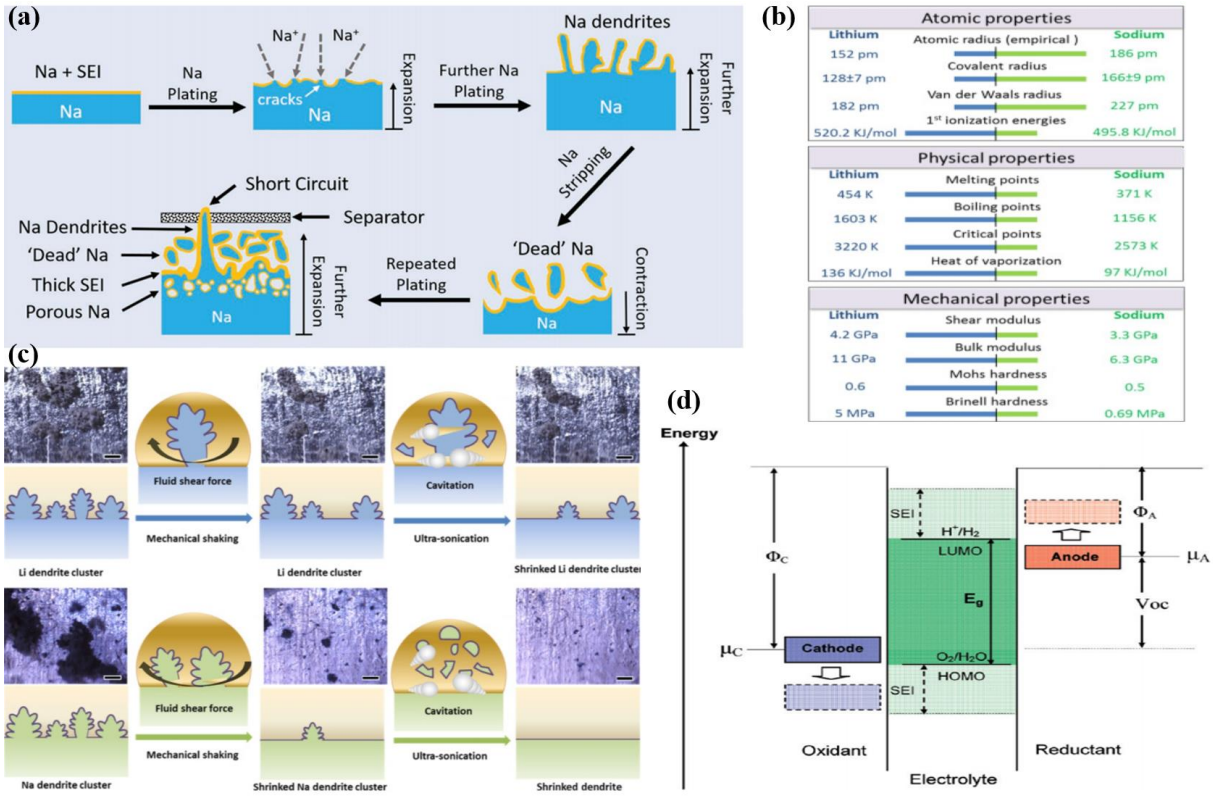

Figure 1. (**a**) Schematic diagram of problems with sodium metal anodes during plating/stripping processes [55]. (**b**) Various properties of lithium and sodium. (**c**) Mechanically stability under quasi-zero electrochemical field for Li and Na dendrites [49]. Reprinted with permission. Copyright 2018, Elsevier. (**d**) Schematic showing the energy levels of the electrodes with electrolyte [51]. Reprinted with permission. Copyright 2009, ACS.

2.3. Large volume changes during plating/stripping processes

During the plating/stripping process, volume expansion is a common issue in secondary batteries. It has been reported that the relative volume change of graphite in lithium-ion batteries is approximately 10%, while the relative volume change of silicon anodes can reach about 400% [58,59]. Unlike embedded anodes such as graphite or alloy-type anodes such as silicon, the volume expansion of sodium metal-an anode with no substrate-is theoretically unlimited. The significant volume change generates mechanical stress that causes SEI film cracking and creates cracks with low diffusion energy barriers for Na^+, which promotes dendrite growth [60]. Simultaneously, the large volume expansion leads to internal stress variations and electrode pulverization, reducing the structural stability of the battery and severely affecting its cycling performance [61]. Therefore, establishing an electrode-electrolyte interface with good flexibility to accommodate the volume changes of sodium metal anodes during plating and stripping is crucial.

3. Construction of electrode-electrolyte artificial interfacial layer

The properties of the SEI layer play a decisive role in achieving a stable Na- metal anode [34,62]. Unfortunately, the natural SEI layer formed by the sodium metal anode and the electrolyte is uneven and brittle, making it ineffective at suppressing dendrite formation. This not only reduces the battery's Coulombic efficiency but also poses safety risks [63]. Therefore, it is crucial to optimize the properties of the SEI by modulating its composition. An ideal SEI layer should possess good chemical and electrochemical stability (to minimize side reactions), excellent ionic conductivity and electrical insulation (to prevent the formation of sodium nuclei on the SEI), uniform electric field distribution and low diffusion barriers (to ensure uniform Na^+ deposition), and good flexibility and mechanical strength (to accommodate volume changes and prevent dendrite growth) [64,65]. To achieve these properties, researchers have been exploring the design of artificial interfacial layers on alkali metal anodes. This work is of great significance for realizing high-performance, safe, and stable sodium metal anodes [61]. Depending on the composition, artificial interfacial layers can be classified into inorganic, organic, and inorganic-organic composite layers.

3.1. Inorganic artificial interface layer

Inorganic SEI layers have relatively high Young's modulus and ionic conductivity, which allows them to effectively guide Na^+ transport while suppressing the growth and development of dendrites. These properties make inorganic SEI layers widely used in the regulation of sodium metal anodes [66].

Research on lithium metal batteries has shown that LiF can effectively stabilize lithium metal anodes and guide the uniform deposition of lithium. This concept can be applied to the study of sodium metal batteries, leading to numerous reports on constructing NaF-rich artificial interfacial layers to protect sodium metal anodes [64,67]. For example, Cui *et al.* utilized the simple electrolyte $NaPF_6$ (sodium hexafluorophosphate) to form an inorganic SEI protective layer primarily composed of Na_2O and NaF on sodium metal, providing the first demonstration of NaF's stabilizing effect on sodium. This protective layer has a high Young's modulus, effectively suppressing dendritic development. Electrochemical tests showed that without any additional treatment methods, the average Coulombic efficiency reached 99.9% over 300 cycles at a current density of 0.5 mA cm^{-2}. The average voltage hysteresis between plating and stripping was between 13.3 and 19.5 mV, with no dendrite growth observed on the surface after cycling [18]. Recently, Cheng's team reported a simple method for constructing tunable fluorine-based artificial SEIs through the fluorination reaction of alkali metals with mild organic fluorinating reagents (Figure 2a). The fluorine-based artificial SEI layers were created by immersing lithium metal in pure triethylamine trihydrofluoride (TREAT-HF), sodium and potassium metals in triethylamine hydrogen trifluoride solutions. Scanning electron microscopy (SEM) revealed that after cycling, a significant number of dendrites with a porous structure formed on the bare sodium anode, making the surface rougher (Figure 2b–d). In contrast, the solution-treated sodium anode exhibited a much smoother surface with no dendrite formation after cycling (Figure 2e–g). The immersion time

is closely related to the thickness of the fabricated SEI coating, and it can be adjusted to achieve the most suitable SEI morphology and thickness, leading to higher performance. It was also observed that the thickness of the deposition on bare alkali metal was twice that of the deposition after artificial SEI modification. This significant difference can be attributed to the uniform and dense structure of the artificial SEI. The abundant grain boundaries in the artificial SEI layer facilitate the efficient transport of alkali metal ions and provide high mechanical strength with a bulk modulus of 70 GPa [68]. The above methods improved the stability of sodium metal anodes, but suffered from the drawbacks of high cost and toxicity. Xu *et al.* employed a simple and cost-effective strategy by adding polytetrafluoroethylene (PTFE) micropowder to molten sodium, forming an *in-situ* NaF-rich protective layer on the sodium metal surface (Figure 2h). This resulted in uniform sodium deposition and effectively suppressed dendrite growth. In both ether-based and carbonate-based electrolytes, full cells using $Na_3V_2(PO_4)_3$ cathodes maintained a Coulombic efficiency of 99% after long cycles [69]. Recently, Damircheli and colleagues developed a durable fluorinated artificial SEI layer on the surface of sodium metal by adding various weight ratios of tin fluoride to a dimethyl carbonate solution (Figure 2i). This method is simple and cost-effective, and the resulting protective layer effectively stabilized the surface of the sodium metal, significantly enhancing its cycling stability. At a current density of 0.25 mA cm^{-2}, the artificial SEI layer dramatically increased the lifespan of Na-metal symmetric cells compared to untreated sodium, with a cycling stability time exceeding 700 hours [70].

Other elements in the halide group can also be considered for constructing artificial SEI layers for sodium metal anodes. For instance, Choudhury's team used joint density functional theory to show that the binding energy of sodium-bound atoms depends on their position on the sodium halide surface (Figure 3b). They also found that NaBr has the lowest ionic interfacial diffusion barrier (Figure 3a), which promotes faster ion diffusion and uniform deposition while suppressing dendrite growth. Subsequent experimental results confirmed that a symmetric cell with NaBr-coated electrodes maintained a Coulombic efficiency exceeding 99% and a stable voltage plateau after 250 cycles in a liquid electrolyte [71]. Subsequently, Wang's team attempted to form an *in-situ* NaI artificial SEI layer on sodium metal anodes (Figure 3c). The formation of the *in-situ* NaI SEI layer resulted in sodium metal batteries exhibiting extremely high cycling stability (over 2200 cycles at 2 C), high capacity (up to 210 mAh g^{-1} at 0.5 C), a high discharge voltage plateau (> 2.7 V), and low overpotential. DFT calculations indicated (Figure 3d–g) that the diffusion barrier of NaI is lower than that of NaF, allowing for continuous and rapid Na^+ deposition and preventing the formation of Na dendrites [72].

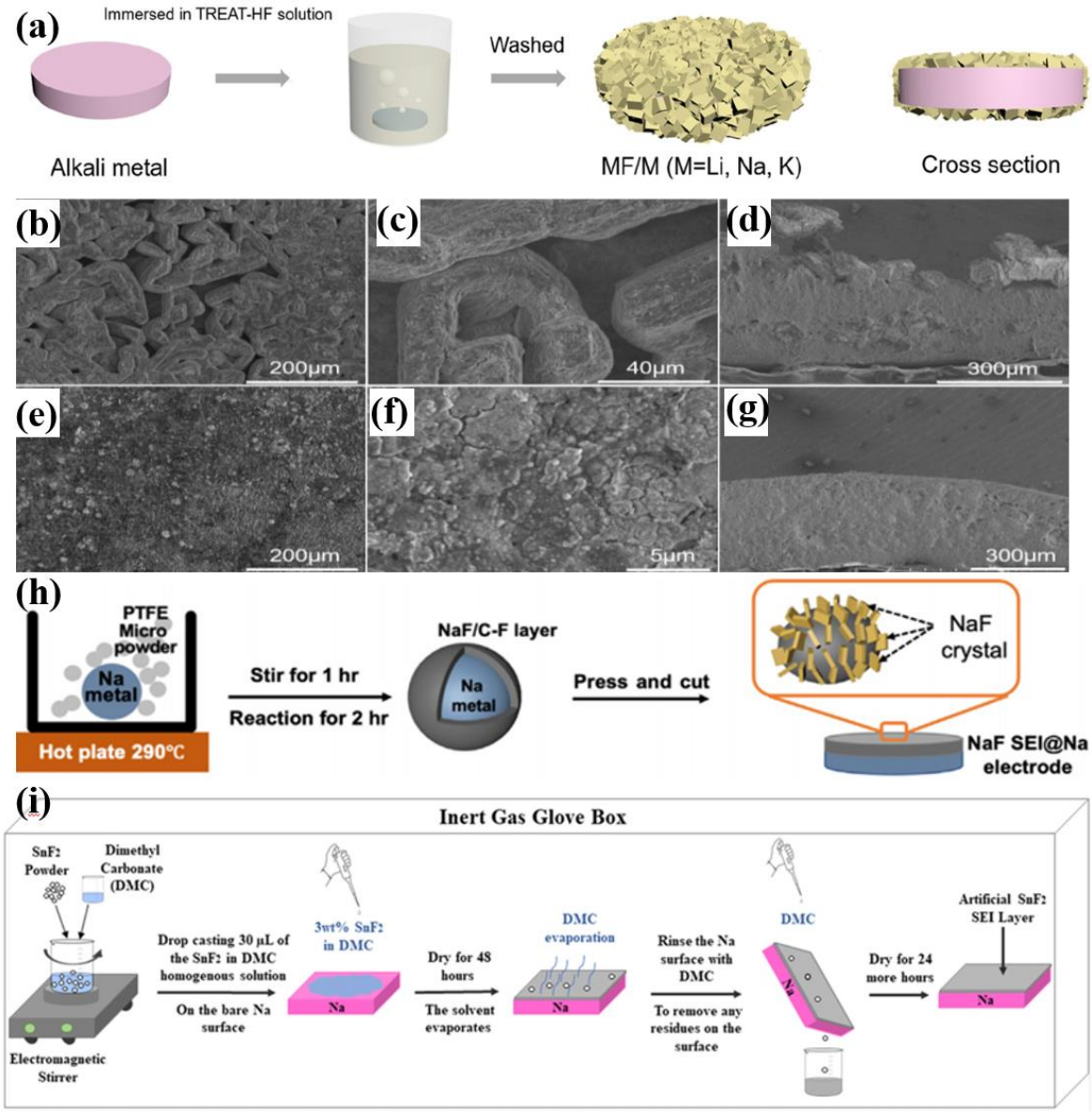

Figure 2. (**a**) Schematic diagram of alkali metal anode fluoridation method. SEM images of bare Na at (**b**) low, (**c**) high and (**d**) its cross-sectional view after 30 cycles cycle at a current density of 3 mA cm^{-2}. SEM images of Na/a-SEI at (**e**) low, (**f**) high and (**g**) its cross-sectional view after 30 cycles cycle at a current density of 3 mA cm^{-2} [68]. Reprinted with permission. Copyright 2009, ACS. (**h**) Schematic diagram of NaF production process [69]. Reprinted with permission. Copyright 2022, Elsevier. (**i**) Formation of SEI layer on Na-metal surface by artificial SnF_2 coatings [70]. Reprinted with permission. Copyright 2023, ACS.

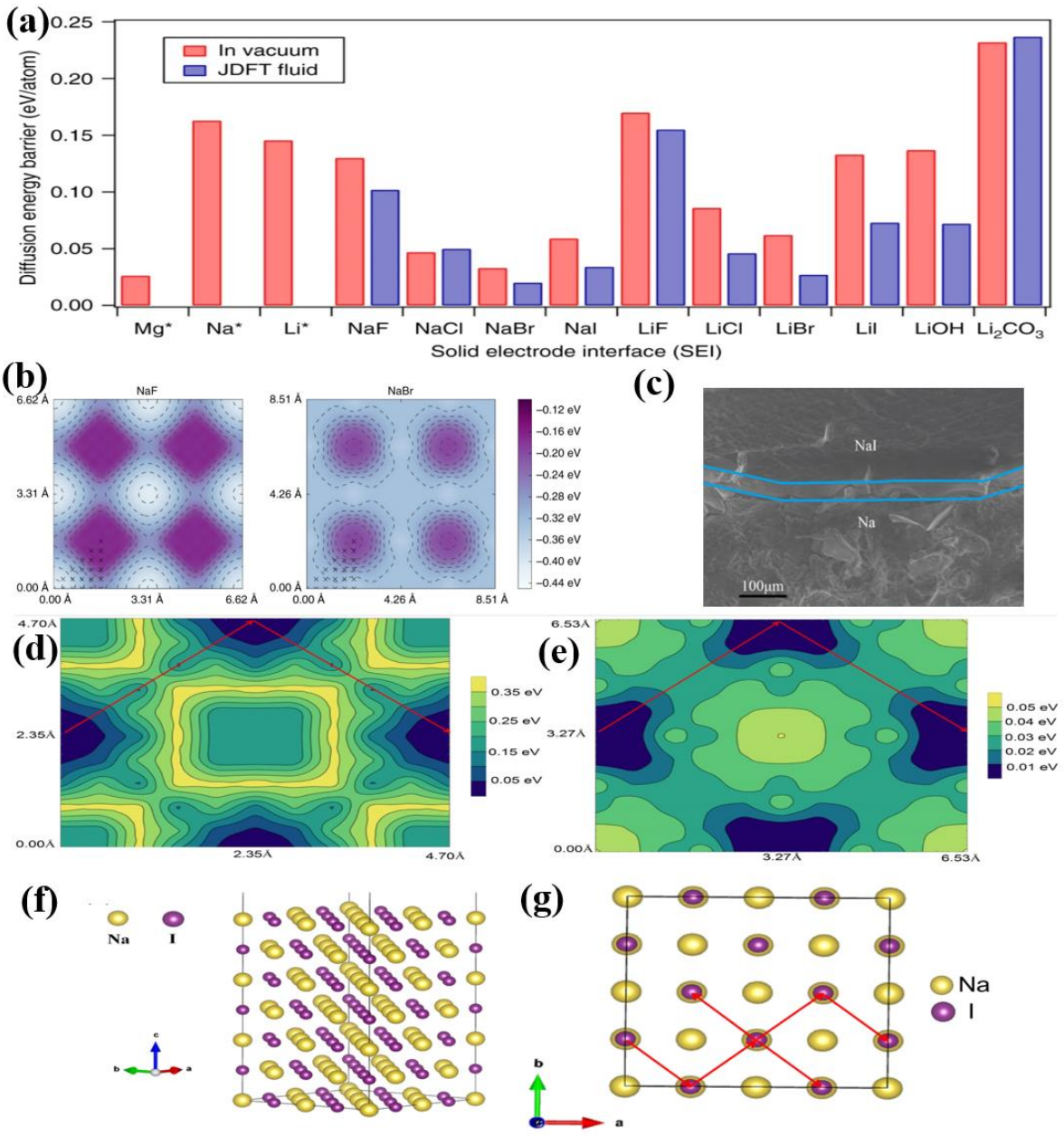

Figure 3. (**a**) Diagram illustrating the diffusion barriers of magnesium, sodium, and lithium atoms on their surfaces. (**b**) Surface binding energy vs. binding location of NaF (left) and NaBr (right) [71]. (**c**) SEM images of metal Na anodes treated with 2-iodopropane. (**d**–**g**) Surface diffusion barriers obtained by theoretical calculations using the density functional theory method: The calculated surface binding energy vs. binding site: (**d**) Na adatoms on NaF surfaces. (**e**) Na adatoms on NaI surfaces. (**f**) Schematic for the NaI slab and (**g**) the transport paths of Na adatoms on a NaI surface [72]. Reprinted with permission. Copyright 2019, Elsevier.

In addition to protective layers made of NaX (X = F, Cl, Br, I), researchers have also explored artificial protective layers composed of other inorganic components. Wang *et al.* used a mechanical kneading method to uniformly embed $NaNO_3$ into a sodium metal framework, creating a Na/$NaNO_3$ hybrid foil electrode (Figure 4a,b). During battery cycling,

a stable SEI layer containing NaN_xO_y and Na_3N was formed, facilitating high-speed ion transport. Additionally, the continuous availability of $NaNO_3$ addresses the low solubility issue of SEI stabilizers [73]. Shi's team initially employed a red phosphorus pretreatment process, which involves repeatedly grinding red phosphorus powder on the surface of sodium metal at room temperature to form a Na_3P layer (Figure 4c). This layer exhibits strong ionic conductivity and excellent mechanical durability. Its low energy barrier (11.0 kJ mol^{-1}) and high ionic conductivity (approximately 0.12 mS cm^{-1}) effectively facilitate the migration of Na^+ ions within the electrode, promote uniform deposition, and suppress side reactions. Atomic force microscopy revealed that its Young's modulus is significantly higher than that of bare sodium (Figure 4d,e), successfully inhibiting dendrite growth. Due to these advantages, symmetric cells protected by the Na_3P interfacial layer demonstrate significantly better cycling performance compared to untreated bare sodium electrodes [74]. Additionally, Luo *et al.* selected a Na_3P layer, known for its abundant ion conduction channels, and a NaBr layer, characterized by a low surface diffusion barrier and wide bandgap, through theoretical calculations. The combination of these two components as an artificial protective layer addresses the poor cycling performance typically caused by the high bulk diffusion barrier of NaBr and the high conductivity of Na_3P. A composite SEI layer of NaBr and Na_3P was formed on the surface of metallic Na through the spontaneous reaction between metallic Na and phosphorus tribromide (PBr_3). Cryo-TEM observations revealed crystalline surfaces of NaBr, Na_3P, and Na_3PO_4 (Figure 4f), which provide pathways for sodium ion transfer. Under this protective layer, the Na electrode surface remained smoother even after plating 5 mAh cm^{-2} (Figure 4g), whereas the bare sodium surface showed significant dendrite growth (Figure 4h). This composite interface meets multiple requirements for an ideal SEI layer and ensures long-term stability for Na metal anode in carbonate electrolytes. The assembled symmetric cells, as well as the full cells using $Na_3V_2(PO_4)_3$ as the cathode, both demonstrated excellent stability [38].

The electrochemical performance of sodium metal anodes can also be significantly enhanced by introducing sodium-philic metals on the sodium metal surface to form a sodium-metal alloy interface. Lv's team was the first to report a sodium-gallium alloy coating to improve the stability of sodium anodes [75]. Gallium metal, with a low melting point of 30 ℃, easily alloys with sodium metal (Figure 5a). XRD results (Figure 5b) show that the alloying reaction between Na and Ga produces $Na_{22}Ga_{39}$. The alloy protective layer possesses a high Young's modulus and sodiphilicity. In carbonate electrolytes, symmetric cells (NGAL-Na||NGAL-Na) made with the alloy-protected sodium metal electrodes demonstrated an expected lifespan of 468 hours at 6 mAh cm^{-2}. Subsequently, a group of alloy-type interfaces (Na-In, Na-Bi, Na-Zn, Na-Sn) were investigated as artificial SEI layers by Moorthy *et al.* These high sodiphilicity SEI components were prepared on the surface of Na alloys, forming protective alloy layers with low energy barriers, which promote the rapid diffusion of sodium ions across the interface. Density functional theory (DFT) calculations (Figure 5c–f) indicate that, compared to bare Na, the reduced surface energy of the alloy coating is a key factor in promoting ion migration at the interface. The authors further explained the differences in electrochemical performance among various alloy-protected layers. Specifically, the Na-In

alloy-protected interface exhibited lower adsorption and diffusion energy barriers for Na, which facilitates a highly reversible Na plating/stripping process. This interface achieved a stable cycling time of approximately 790 hours at 2 mA cm^{-2}; significantly higher than the cycling time of unmodified Na metal (100 hours). Additionally, full cells assembled with $Na_3V_2(PO_4)_3$ as the cathode demonstrated improved cycling performance at high current densities (5 mA cm^{-2}) and high capacities (10 mAh cm^{-2}) [76].

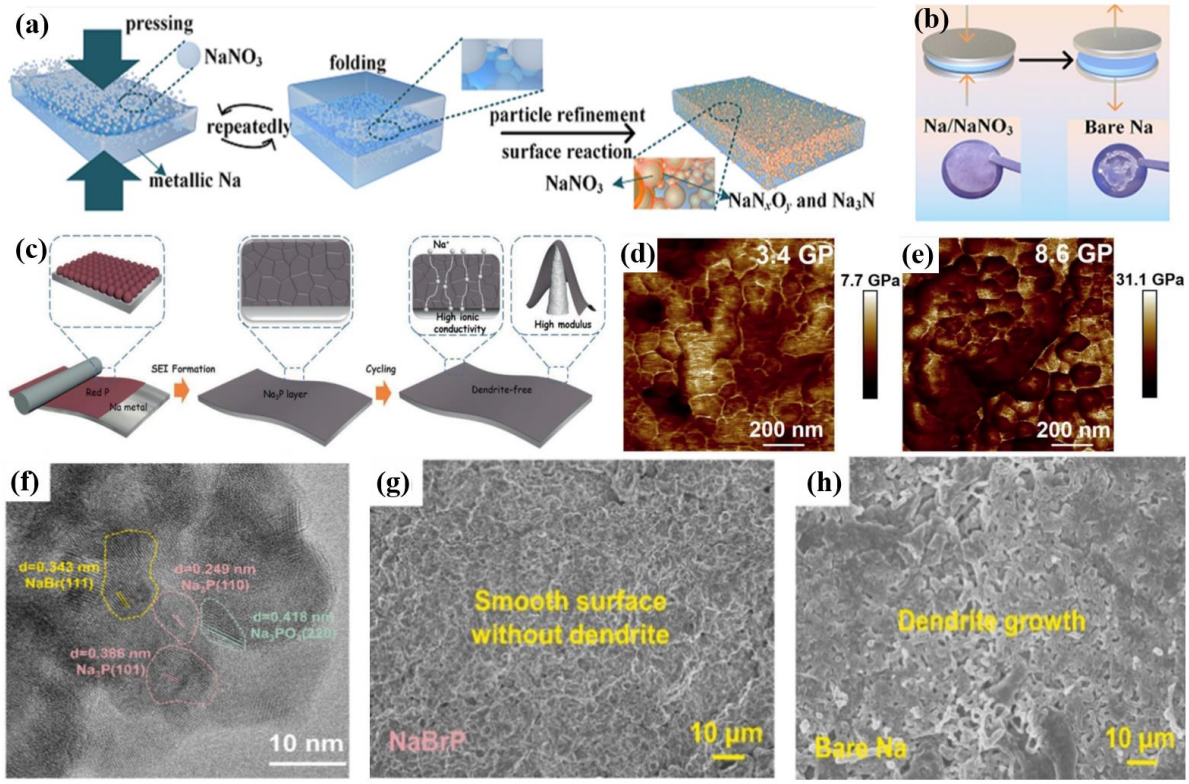

Figure 4. (**a**) Schematic diagram of $Na/NaNO_3$ composite foil prepared by mechanical kneading and (**b**) assembled button cell [73]. Reprinted with permission. Copyright 2021, ACS. (**c**) Preparation process of Na_3P layer on sodium metal anode and its advantages. (**d,e**) The distribution of Young's modulus on the surface of (**d**) bare Na and (**e**) Na_3P@Na anodes [74]. Reprinted with permission. Copyright 2020, Wiley-VCH. (**f**) High-resolution images of the microstructure of NaBrP coatings. (**g,h**) top views NaBrP/Na (**g**) and Na electrode (**h**) after plating 5 mAh cm^{-2} of Na at 1 mAh cm^{-2} [38]. Reprinted with permission. Copyright 2022, Elsevier.

Recently, Geng's team successfully generated a heterogeneous interlayer of $Na_2Se/Na_{15}Sn_4$ by conducting an *in-situ* reaction on Na metal surfaces coated with SnSe nanosheets (Figure 6a). SEM images and the corresponding energy dispersive spectroscopy (EDS) analysis indicate that Sn and Se elements are uniformly distributed across the Na anode, forming a protective layer with a thickness of about 60 μm (Figure 6b). Compared to single components (Sn or Se), the SEI layer formed from the spontaneous *in-situ* reaction between SnSe and Na tightly adheres to the Na metal. This ensures rapid diffusion and uniform electric field distribution during Na^+ plating or stripping processes. The high

Young's modulus (13.2 GPa) of this heterogeneous interface also provides excellent mechanical strength, preventing dendrite growth and penetration. DFT calculations were conducted to determine the adsorption energy of Na^+ on both the Na metal and $Na_2Se/Na_{15}Sn_4$ surfaces, as well as the diffusion energy barriers of Na^+ within the protective layers of different compositions. The results indicate that the heterogeneous $Na_2Se/Na_{15}Sn_4$ protective layer exhibits a higher affinity for Na^+ compared to metallic sodium. The energy barrier for Na^+ transport along the Na_2Se (100) crystal surface is approximately 0.1467 eV, which is significantly lower than that of the typical SEI component NaF (0.2671 eV). Thanks to this protective layer, symmetrical sodium batteries can sustain continuous cycling for 2400 hours at 0.5 mA cm^{-2}. Additionally, the Na/Se||NFM(333) pouch cell achieved at least 1800 cycles at a high current density of 2 A g^{-1} [77].

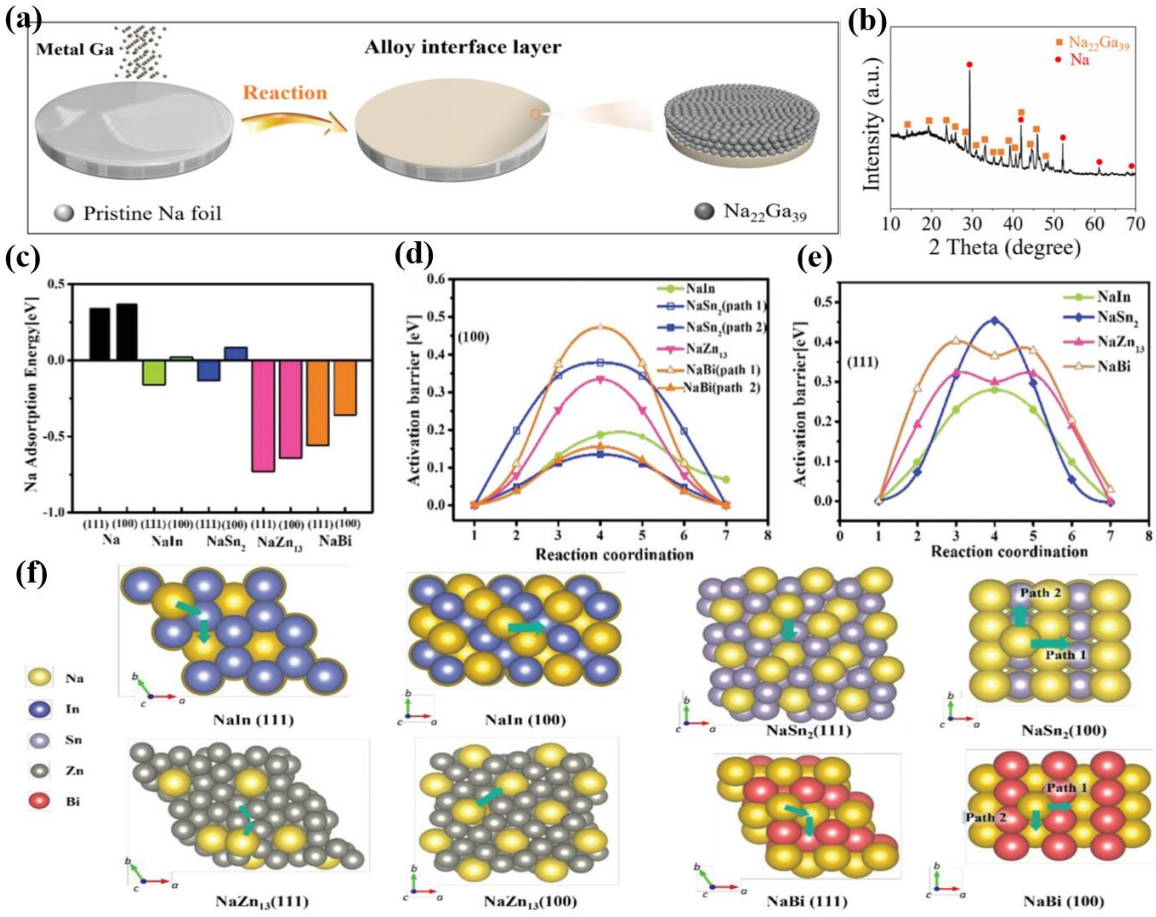

Figure 5. (**a**) Schematic diagram of Na-Ga alloy layer (NGAL-Na) prepared by rolling metallic Ga on Na metal. (**b**) X-ray diffraction (XRD) pattern of Na-Ga [75]. (**c**) Na adsorption energy and diffusion activation barrier for NaIn, $NaSn_2$, $NaZn_{13}$ and NaBi. The activation barrier for (100) plane is shown in the left panel of (**d**), and the activation barrier for (111) plane is shown in the right panel of (**e**), (**f**) the Na diffusion pathway of each alloy [76]. Reprinted with permission. Copyright 2023, Wiley-VCH.

The aforementioned treatments are relatively simple and cost-effective. However, it is challenging to obtain a uniform and intact film through the chemical interactions between

sodium and other materials, which may result in uneven sodium ion flux or localized deposition [63]. In addition to chemical pretreatment methods for achieving a stable SEI layer, there are also some physical deposition techniques available. For example, atomic layer deposition (ALD) is a gas-phase thin film deposition process that can produce highly uniform and consistent films, which protect metals from electrolyte corrosion [64,78]. Sun's team has demonstrated that ultra-thin ALD coating technology can be used as a protective layer for lithium metal anodes. Following this, they also applied ALD technology to sodium metal anodes. By using trimethylaluminum (TMA) and water (H_2O) as precursors, they directly deposited an ultra-thin Al_2O_3 protective layer on Na foil at 85 ℃, effectively suppressing the growth of Na dendrites (Figure 6c). They found that the thickness of the Al_2O_3 layer has a significant impact on the cycling life of the battery. Sun's team further developed a two-step ALD deposition method that does not require alkali metal precursors to synthesize alkali metal cation conductive interfaces (Figure 6d). This method addresses the issue of poor ionic conductivity in most alkali metal ALD coatings. The $LiAlO_x$/$NaAlO_x$ coatings obtained using this two-step method are uniform, smooth, and well-controlled. The optimized ionic conductive coatings can significantly enhance the electrochemical performance of Li and Na metal anodes in both symmetrical and full batteries (Figure 6e,f), demonstrating the versatility of this method [79].

Overall, inorganic interface protective layers generally exhibit high shear modulus and ionic conductivity, which effectively suppress dendrite growth and promote uniform Na deposition. However, they have poor flexibility and struggle to accommodate the stress caused by volume changes in the Na anode during charge and discharge, leading to potential cracking. Additionally, protective coatings constructed through various methods have their own specific issues. For example, Na-X (halogens, alloys, or other elements) protective layers formed via *in-situ* reactions are often created through techniques such as drop-casting, scraping, or dipping. While these methods are relatively simple and practical, they do not allow for precise control over the uniformity and thickness of the interface, necessitating further improvements to achieve a more uniform and dense layer. Constructing protective layers using multiple inorganic components (such as NaBr-Na_3P, Na_2Se-$Na_{15}Sn_4$, NaCl-Na alloys, *etc.*) can also offer excellent electrochemical performance. However, the interactions or adverse reactions between different components have not been thoroughly validated. More refined experiments are needed to explore these issues to better design the composition of protective layers. ALD technology produces more uniform and controllable thicknesses of protective layers but is more expensive. Balancing cost, performance, and preparation difficulty is essential to facilitate commercialization.

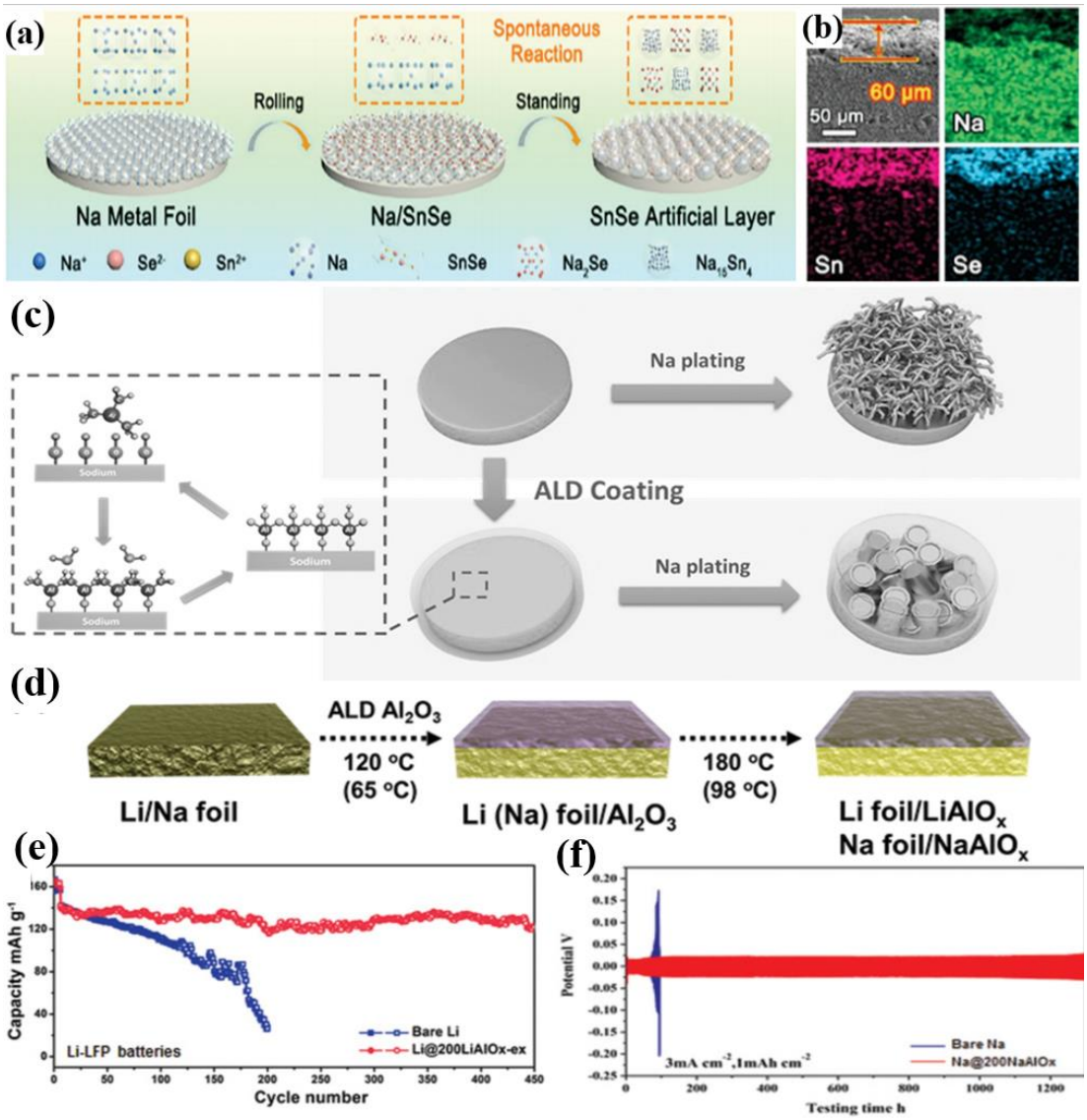

Figure 6. (**a**) Schematic diagram of the synthesis process of Na/SnSe electrode. (**b**) SEM images of Na/SnSe electrodes and their corresponding EDS profiles [77]. Reprinted with permission. Copyright 2024, Wiley-VCH. (**c**) Schematic diagram of ALD deposited alumina film stabilized sodium metal anode [26]. Reprinted with permission. Copyright 2017, Wiley-VCH. (**d**) Schematic of a two-step strategy for preparing ion-conducting layers on Li or Na metal anodes. (**e**) Cycling performances of full cells (C/$LiFePO_4$ as the cathode) using bare Li foil and Li@200LiAlOx-ex as anode electrode at 1 C. (**f**) The overpotential of Na/Na symmetric cells using bare Na foil and Na@200NaAlOx under the conditions of 3 mA cm^{-2} /1 mAh cm^{-2} [79]. Reprinted with permission. Copyright 2022, Wiley-VCH.

3.2. Organic artificial interface layer

Unlike inorganic protective layers, organic protective layers can be designed at the molecular level [80]. In addition, the flexibility of the organic protective layer can effectively address mechanical stresses caused by volume changes. Their functional groups can further enhance

the adhesion of the protective layer and promote more uniform Na deposition [66]. Therefore, organic protective layers might additionally serve to strengthen sodium-metal anodes.

An organic protective layer can also be constructed through chemical pretreatment. Zhu *et al.* created an organic sulfide-rich (PhS_2Na_2) protective layer with a thickness of about 5 micrometers on the top layer of a metallic sodium anode using chemical pretreatment (Figure 7a,b). This protective coating successfully inhibited the formation of sodium metal dendrites in carbonate electrolytes, achieving 400 cycles (800 hours) of sodium metal electrodeposition and stripping at a current density of 1 mA cm^{-2}. Additionally, DFT calculations show that PhS_2Na_2 has the lowest surface binding energy compared to other conventional SEI components (CH_3ONa, CH_3OCO_2Na and Na_2CO_3). This lower binding energy leads to higher ionic conductivity, which facilitates the transport of Na^+ ions within the SEI layer (Figure 7c) [81]. Lu's team used 1,3-dioxane to pretreat the sodium metal anode and prepared an effective protective layer (Figure 7d). This protective layer enables rapid sodium ion transport with low charge transfer resistance, reducing dendrite growth. Digital microscopy images show that, compared to bare Na, the presence of the protective layer significantly reduces gas evolution at the interface (Figure 7e,f). The assembled symmetric cell achieved an ultra-long cycle life of at least 2800 hours at a current density of 1 mA cm^{-2} and a cycling capacity of 1 mAh cm^{-2}. A full cell with $Na_3V_2(PO_4)_3$ as the cathode also demonstrated excellent electrochemical performance [82]. Recently, Wang *et al.* constructed an artificial formate sodium (HCOONa) layer on the surface of sodium metal through a solid-gas reaction (Figure 7g). Scanning electron microscopy and other characterization techniques revealed that the HCOONa interface effectively suppressed dendrite growth, reduced the exposure of sodium to the electrolyte, and minimized side reactions. The assembled Na|NVP (sodium vanadium phosphate) battery demonstrated significant improvements in high-rate performance (with a capacity of up to 98.7 mAh g^{-1} at 10 C) and good cycle performance (with an energy density of up to 101.2 mAh g^{-1} after 800 cycles at 2 C). In addition, the anodeless sodium metal battery, with a protective layer of HCOONa formed on the current collector, also exhibited excellent cycling performance. A full battery, with a monolayer of sodium oxalate constructed on copper foil as the anode and NVP as the cathode, was able to stably cycle for 400 cycles at 0.5 C [83].

Polyvinylidene fluoride (PVDF) has excellent dielectric properties and is an ideal material for stabilizing sodium metal anodes [84]. Ma's team prepared PVDF films with different structures and compared them with polyethylene oxide (PEO) and polytetrafluoroethylene (PTFE) films (Figure 7h). They found that the f-PVDF film, due to its non-permeable structure and inherent properties, exhibited the highest ionic conductivity. Its fibrous structure facilitates electrolyte uptake, while its strong polar functional groups and good affinity with the electrolyte promote uniform sodium ion flux and deposition. The f-PVDF film performed well in Na-O_2 batteries, showing high rate capability and cycle life (about 87 cycles) [85]. Later, Hou *et al.* constructed a PVDF protective layer on the surface of a copper current collector using scalable blade coating technology, achieving dendrite-free Na plating/stripping. The PVDF coating formed a smooth and stable SEI on the PVDF-Cu current collector, successfully suppressing the adverse reactions between the Na metal anode and the

electrolyte. X-ray photoelectron spectroscopy (XPS) studies revealed that the SEI on the PVDF-Cu collector mainly consists of NaF, Na_2O_2 and RCH_2ONa (Figure 7i). The SEI possesses a high shear modulus and is rich in NaF, which endows the full cell with excellent electrochemical performance, including a long lifespan of 1200 hours at 1 mA cm^{-2}, an overpotential of approximately 35 mV, and a Coulombic efficiency of about 99.91% after 2000 hours of cycling [86].

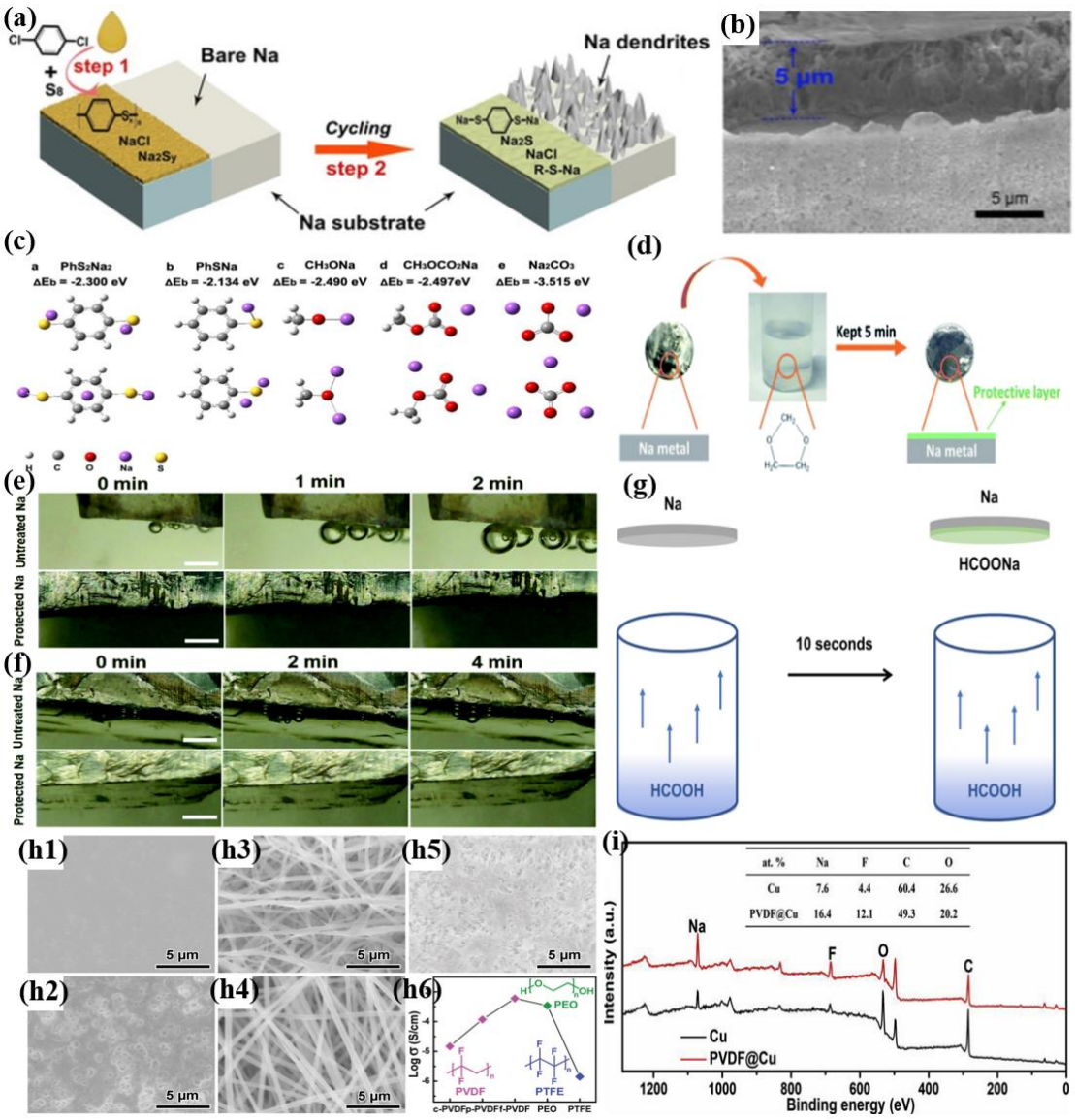

Figure 7. (**a**) Schematic of the preparation of a protective layer of Sodium Benzenedithiolate-Rich on metallic sodium foil. (**b**) SEM image of the protected sodium foil. (**c**) molecular structure, and the binding energy between Na^+ and different SEI components [81]. Reprinted with permission. Copyright 2020, Wiley-VCH. (**d**) Schematic diagram of sodium protection for 1,3-dioxane pretreatment method. (**e,f**) *In situ* digital micrograph images of the cross-sectional surface of untreated Na and protected Na in (**e**) TEGDME solvent and (**f**) the electrolyte (1 M $NaPF_6$ in TEGDME), recorded at different times [82]. (**g**) Schematic diagram of the solid-gas reaction method used to prepare HCOONa-Na [83]. Reprinted with permission. Copyright 2023, Wiley-VCH. (**h**) SEM

image of (**h1**) c-PVDF, (**h2**) p-PVDF, (**h3**) f-PVDF, (**h4**) PEO film, (**h5**) PTFE film, and (**h6**) ion conductivity of these films in 0.5 m $NaCF_3SO_3$/TEGDME electrolyte [85]. Reprinted with permission. Copyright 2018, Wiley-VCH. (**i**) XPS of SEI on Cu collector and PVDF-Cu collector after 5 plating/stripping cycles [86]. Reprinted with permission. Copyright 2020, Elsevier.

Organic protective layers that are easy to form, with a certain degree of viscosity and flexibility, can adhere well to the surface of Na anodes and effectively accommodate the volume changes of the Na anode. However, there are many issues with these layers. Currently, there are few reports on organic protective layers for sodium metal anodes, and they generally have low ionic conductivity and poor mechanical strength, making them ineffective in suppressing the growth of sodium dendrites. Additionally, some organic reagents are toxic and environmentally unfriendly. This requires a more in-depth consideration of these factors to facilitate further development.

3.3. Inorganic-Organic composite artificial interface layer

As previously mentioned, inorganic materials offer the advantages of high shear modulus and ionic conductivity, but they lack flexibility. On the other hand, organic materials possess excellent flexibility but often have lower mechanical strength and poor alkali metal ion mobility [87,88]. Therefore, combining inorganic and organic components is expected to produce a superior SEI layer. If an artificial SEI layer can incorporate the strengths of both inorganic and organic components–exhibiting good mechanical strength, ionic conductivity, and resistance to deformation–it would be more effective in suppressing dendrite formation and accommodating the volume changes during alkali metal plating/stripping, thereby achieving uniform deposition [89].

Organic SEI layers constructed from a single PVDF, as stated earlier, cannot provide good Young's modulus and ionic conductivity. Therefore, researchers have combined the PVDF matrix with other inorganic components to achieve more satisfactory results [90–92]. For example, Jiao *et al.* prepared a free-standing, implantable artificial protective film (FIAPL) by mixing NaF and PVDF powder. The combination of NaF's high shear modulus and PVDF's good flexibility effectively suppresses the growth of Na dendrites while better accommodating the mechanical stress caused by the anode's volume changes during charge and discharge cycles (Figure 8a). They found that the protective layer with a mass ratio of 4:1 for NaF and PVDF exhibited the best performance (Figure 8b,c). The Na symmetric cell assembled with this protective layer demonstrated up to 1200 hours of cycling life at a current density of 0.25 mA cm^{-2} [93]. Huang's team used blade coating technology to cover a copper collector with an artificial composite protective layer made of Sn-PVDF (PSN@Cu) (Figure 8d). Sn has been reported to have a high Young's modulus (46.9 GPa) [94] and good affinity for sodium, which facilitates the rapid transport of sodium ions [95] and compensates for the shortcomings of using a single PVDF component. The results from electrochemical impedance spectroscopy (EIS) showed that the interfacial resistance of the bare copper current collector significantly increased after 100 cycles (14.96 Ω to 256.6 Ω), whereas the interfacial

resistance of the PSN@Cu exhibited much smaller fluctuations (9.04 Ω to 24.48 Ω) (Figure 8e). This indicates that the modification formed a stable SEI, suppressing adverse effects. SEM results showed that after 100 cycles, large dendrites formed on the surface of the bare copper, while the PSN@Cu remained dense and smooth, with no dendrite growth observed (Figure 8f) [91]. Zhang and colleagues constructed an organo-metallic protective layer of PVDF and Bi on a copper collector (PB@Cu). The Bi-PVDF electrode with a mass ratio of 2:1 exhibited the best electrochemical performance (Figure 8g). Compared to bare copper, the cells with this protective layer showed a significant improvement in Coulombic efficiency. The PB@Cu demonstrated much less capacity decay after 150 cycles, which was significantly higher than that of the bare copper current collector(Figure 8h) [96].

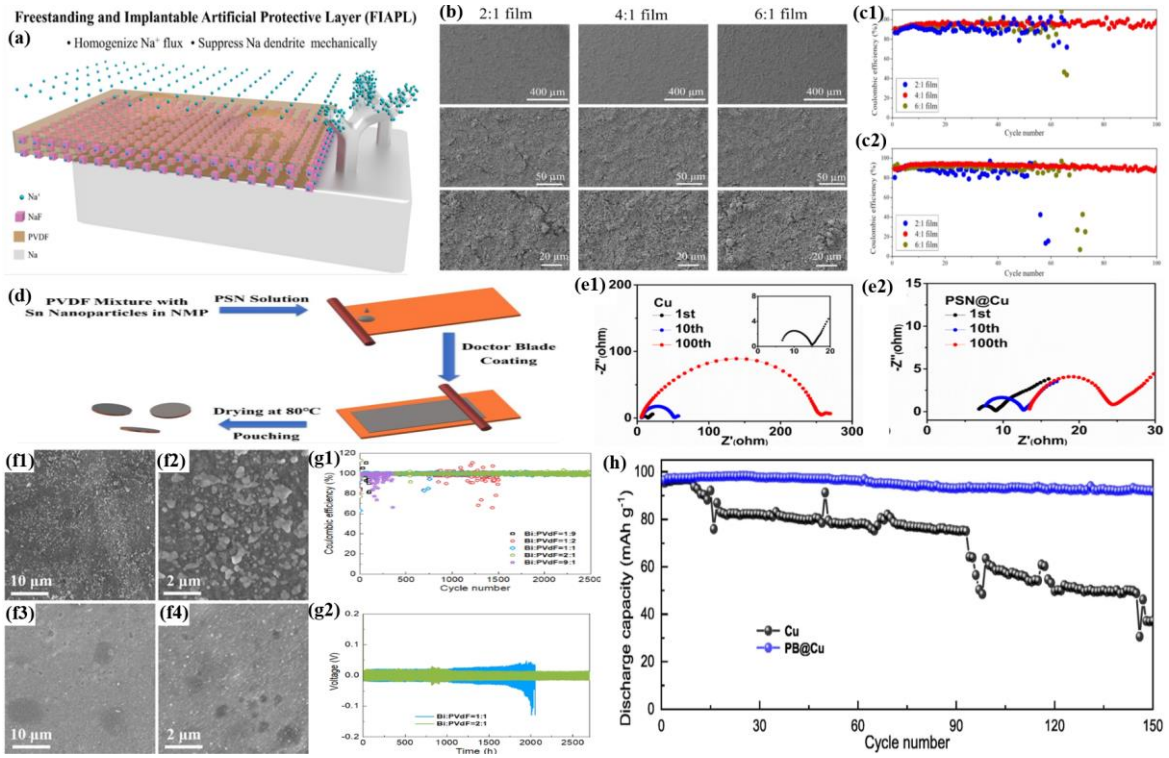

Figure 8. (**a**) Schematic diagram of the working mechanism of FIAPL. (**b**) SEM images of FIAPL with different NaF to PVDF mass ratios. (**c**) Coulombic efficiency plots of NaF and PVDF for Na||Al cells at different mass ratios: (**c1**) at 0.25 mA cm^{-2} / 0.5 mAh cm^{-2} (**c2**) at 0.5 mA cm^{-2}/ 0.5 mAh cm^{-2} [93]. Reprinted with permission. Copyright 2020, ACS. (**d**) Schematic of the preparation of PSN@Cu collectors. (**e**) EIS of (**e1**) bare Cu and (**e2**) PSN@Cu collector after 1, 10 and 100 cycles at 2 mA cm^{-2} with a cycle capacity of 2 mAh cm^{-2} [91]. Reprinted with permission. Copyright 2020, ACS. (**f**) SEM images after cycling: f1-f2) Bare Cu and f3-f4) PSN@Cu collector at 2 mA cm^{-2} / 2 mAh cm^{-2}. (**g**) Electrochemical performance of Cu collectors with different Bi-PVDF ratios: (**g1**) Coulomb efficiency for 1 mA cm^{-2} with fixed cycling capacity of 1 mAh cm^{-2}, (**g2**) voltage profile for 1 mA cm^{-2} with fixed cycling capacity of 1 mAh cm^{-2}. (**h**) Cycling stability of NPV/Cu and NPV/PB@Cu full cells [96]. Reprinted with permission. Copyright 2022, Elsevier.

Apart from PVDF-inorganic components, other organic solutions and inorganic components can also form stable hybrid SEI layers on the surface of sodium metal. For example, Peng and colleagues cast a mixture of ground sodium-potassium (Na57K) alloy and polytetrafluoroethylene (PTFE) nanoparticles onto a collector and used a one-step *in-situ* method to induce PTFE crosslinking on the surface of the sodium metal, constructing a three-dimensional artificial SEI framework with high mechanical strength. The *in-situ* formed crosslinked composite on the alkali metal surface not only possesses high alkali metal ion conductivity due to the presence of metal fluorides but also inherits the excellent mechanical strength of PTFE. Compared to traditional two-dimensional structured protective layers, three-dimensional structured protective layers exhibit excellent structural stability during repeated plating/stripping processes, effectively preventing the collapse of the electrode structure (Figure 9a). The symmetric cell can operate stably at a small and stable polarization voltage (0.06 V) for over 1400 hours at a current density of 0.5 mA cm^{-2} and for more than 600 hours at a high current density of 4 mA cm^{-2}. The full cell, using $Na_3V_2(PO_4)_3$ as the cathode, demonstrates excellent capacity retention in dilute electrolytes at different rates (1 C–80.7%, 2 C–76.5%, 3 C–71.5%) [97]. In addition, Liu's team generated an inorganic-organic hybrid SEI layer (IOHL Na) on the surface of sodium metal through the direct reaction of a solution composed of $SnCl_2$ and 4-chloro-2,6-dimethylphenol with the sodium metal (Figure 9b). The XRD results indicated that the inorganic component (IL) is primarily Sn and NaCl, while the organic component (OL) is polyphenyl ether (PPO) (Figure 9c). The combination of inorganic components with high Young's modulus and strong alkali affinity, and organic components with good film-forming ability and flexibility, leads to the formation of a hybrid SEI layer that suppresses dendrite growth and achieves uniform electric field distribution. Additionally, the planar phenyl structure and π-π interactions of the aromatic compounds in the organic components make the entire heterogeneous layer dense and resistant to deformation, effectively preventing the negative effects of volume changes during the cycling process. The symmetric cell can stably cycle for 2000 hours at a current density of 4 mA cm^{-2}. Additionally, this protective layer significantly improves the performance of Na-O_2 batteries, which can stably cycle 90 times at 0.5 mA cm^{-2} / 0.5 mAh cm^{-2}, with relatively small fluctuations in Coulombic efficiency and charge/discharge capacity [98].

In recent years, metal-organic frameworks (MOFs) and covalent organic frameworks (COFs) have developed rapidly. These materials offer advantages such as high surface area, ordered pores, and controllable pore size, which have prompted researchers to investigate their applications in anode materials [99,100]. Qian *et al.* demonstrated that an interface layer based on MOFs can successfully reduce the volume changes during Li deposition and mitigate the formation of excessive SEI. They also found that the MOF-199 layer has a positive effect in protecting sodium metal anodes. SEM images show that a robust MOFs coating covering the copper surface can effectively suppress dendrite growth (Figure 9d). Additionally, the high specific surface area of MOF-199 increases the wettability of the electrolyte (Figure 9e), leading to better electrolyte absorption and contributing to a more uniform ion flux on the anode surface [101]. Miao's team proposed a strategy for *in-situ* modification of the solid-state sodium metal battery surface using liquid MOFs precursors.

They used ZIF-62 as the precursor and evolved it on the sodium ion superconductor solid-state electrolyte (NASICON SSEs) to form a dense liquid MOFs protective layer (Figure 9f). Compared to the rough surface of bare NASICON SSEs, the modified surface is much smoother (Figure 9g), which improves wettability with the Na anode and facilitates a more uniform Na^+ flux transfer at the interface, while avoiding side reactions and dendrite growth. The assembled Na symmetric cell exhibits a critical current density of 1.0 mA cm^{-2}; and the full cell integrated with an NVP cathode also demonstrates excellent rate capability and cycling stability, with up to 500 cycles at 1 C [102].

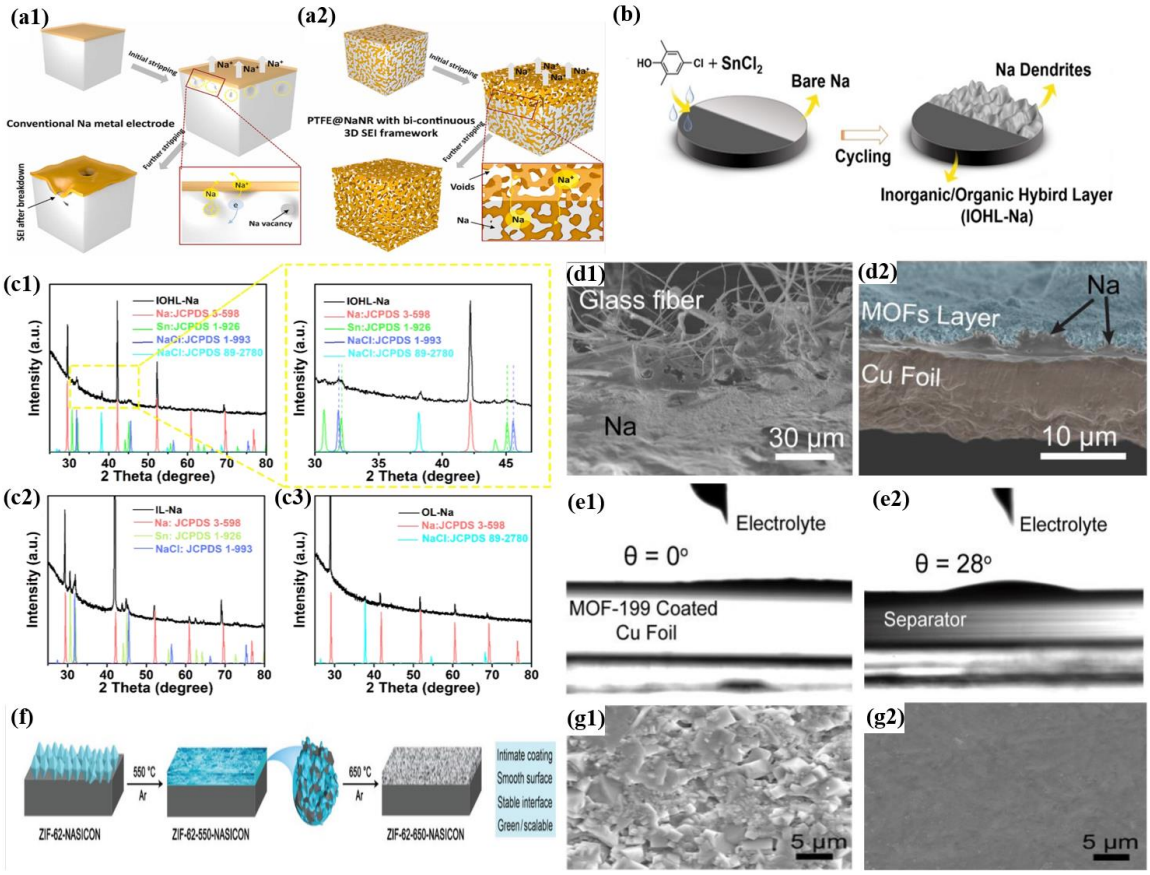

Figure 9. (**a**) The stripping process of Na metal anodes, (**a1**) Conventional Na metal anode with a 2D SEI/metal interface, (**a2**) PTFE@NaNR anode with a bi-continuous 3D SEI framework embedded with nanostructured Na metal [97]. (**b**) Schematic diagram of the preparation of IOHL Na. (**c**) XRD plots of (**c1**) IOHL-Na, (**c2**) IL-Na and (**c3**) OL-Na [98]. Reprinted with permission. Copyright 2023, JOHN/WILEY & SONS, INC. (**d**)SEM cross-sectional images of (d1) pristine Cu and (d2) MOF-199 coated Cu collector electrodes after deposition of 1 mAh cm^{-2}. (**e**) Contact angles of electrolyte (**e1**) on the MOF-199 coated Cu electrode and (**e2**) on the separator [101]. Reprinted with permission. Copyright 2019, Elsevier. (**f**) Schematic diagram of the synthesis process of ZIF-62-650-NASICON. (**g**) SEM top view of (**g1**) bare NASICON and (**g2**) ZIF-62-650-NASICON [102]. Reprinted with permission. Copyright 2021, Wiley - VCH.

Recently, Kang *et al.* demonstrated for the first time that COF materials can stabilize sodium metal anodes. Compared to conventional polypropylene (PP) separators, the COF-based separator significantly suppressed the growth of sodium dendrites (Figure 10a). DFT calculations indicate that the COF separator can decompose PF_6^- in the electrolyte and generate NaF, thereby regulating the SEI composition (Figure 10b). Additionally, test results show that the contact angle of the electrolyte on the COF separator is nearly zero degrees, indicating that the COF separator has excellent affinity for the electrolyte. The SEM images showed that the freestanding COF diaphragm has a staggered structure with a thickness of about 18 μm, which provides a channel for the flow of electrolyte (Figure 10c,d). Therefore, the Na-symmetric cell composed of COF has no dendrite growth and can maintain a stable lifetime of 1500 h at a high current density of 20 mA cm^{-2}. After 5000 cycles at 10 C, the capacity retention rate of the whole battery with COF as the separator was 72% [103].

Molecular layer deposition (MLD) technology is similar to ALD technology mentioned above, and can also be applied to alkali metal anodes to prepare artificial SEI layers. Different from hard and dense ALD coating, MLD coating can add organic components on top of inorganic coating, which has good mechanical properties and flexibility, and has great potential in alkali metal anode protection [104–106]. Sun's team applied the MLD technology for the first time to sodium metal anodes (Figure 10e). MLD alucone films were deposited on the Na-metal surface at 85 ℃ by using trimethylaluminium (TMA) and ethylene glycol (EG) as precursors. They investigated the effect of coating thickness on Na metal electrodes by controlling the number of MLD cycles, finding that 25 MLD cycles yielded the best performance (Figure 10f,g). Additionally, compared to the Al_2O_3 coating applied via ALD, Na coated with alucone demonstrated a longer lifespan and more stable polarization curves, significantly enhancing battery life [107].

Subsequently, Lin *et al.* discovered that combining a polymeric alucone protective film with a solid electrolyte can effectively prevent peroxide crossover in Na-O_2 batteries, significantly enhancing their performance. Specifically, the team used MLD technology to coat the surface of sodium metal with a polymeric aluminum film, but the assembled Na-O_2 battery showed no improvement in electrochemical performance (Figure 11a). This lack of improvement was attributed to the decomposition of the polymeric aluminum layer by reactive superoxide radicals present in the Na-O_2 battery (Figure 11b). However, after replacing the porous glass fiber (GF) diaphragm with a NASICON solid electrolyte, a stable SEI formed on the Na@alucone surface during cycling, eliminating superoxide crossover. As a result, the assembled Na-O_2 full cell exhibited excellent cycling performance, with stable cycling for 325 cycles at 0.2 mA cm^{-2} [108]. Recently, Pirayesh *et al.* combined the ALD process with MLD process to fabricate Al_2O_3-alucone nano-alloys and nanolayered hybrid interfacial layers on Li and Na metal anodes (Figure 11c), and three types of nano-unit structures (ALD Al_2O_3 and MLD alucone) were prepared by modulating the ratio of 1:1 to 2:2 and 5:5, respectively, and further investigated the effect of different thicknesses of each unit structure on the performance by varying the number of deposition cycles. Comparing the samples with different units and thicknesses, the Na@(1ALD-1MLD)10 with Al_2O_3-alucone alloy structure showed the best electrochemical performance at a current density of

3 mA cm^{-2} and a capacity of 1 mAh cm^{-2}. It is notable that the thickness of the SEI layer on the Na surface is approximately 4 nm, while the optimal SEI thickness for Li is 20 nm. The author explains this difference using a cohesive zone model (CZM) to simulate SEI layering (Figure 11d,e). As shown in Figure 11d, when the SEI thickness on Li is uniformly 4 nm, more dendrite growth occurs on Li. Therefore, increasing the thickness of the SEI layer can help resist greater mechanical stress [109].

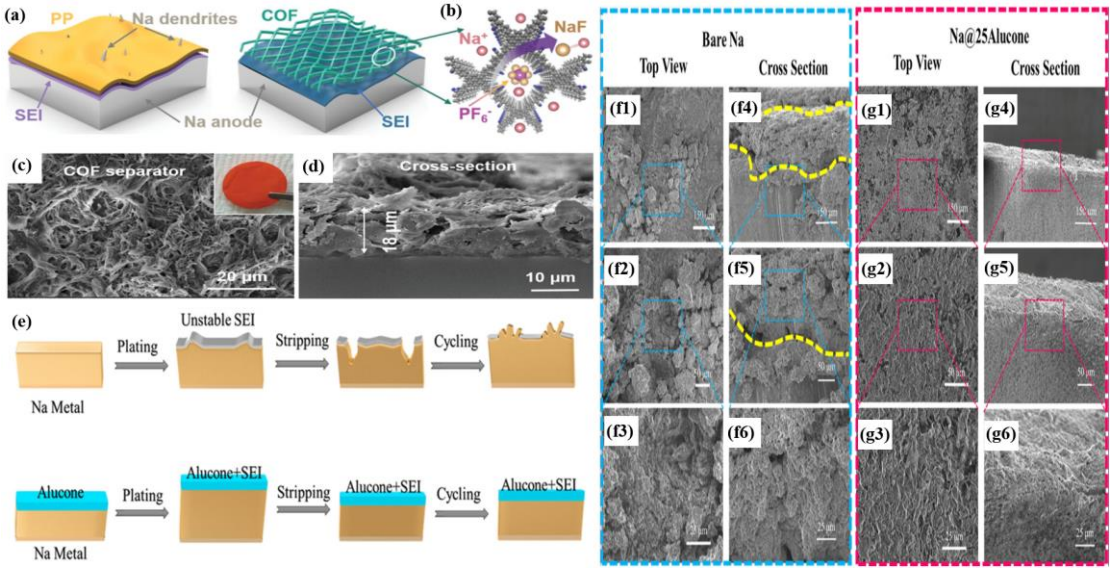

Figure 10. (**a**) Schematic illustration of dendrites formation at a Na anode with a PP separator (left) and a smooth Na anode with a COF separator (right) after cycling. (**b**) The decomposition of PF_6^- to form NaF under the influences of the COF separator. SEM images of the (**c**) surface and the (**d**) cross-section of the COF separator [103]. Reprinted with permission. Copyright 2023, Wiley - VCH. (**e**) Schematic diagrams of Na stripping/plating on bare Na foil and Na foil with MLD alucone coating. (**f**) Top-view and (**g**) cross section view SEM images of bare Na (**f1–f6**) and Na@25Alucone (**g1–g6**) after 10 cycles of stripping/plating at a current density of 1 mA cm^{-2} with the capacity of 1 mAh cm^{-2} [107]. Reprinted with permission. Copyright 2017, ACS.

Ideally, an inorganic-organic composite protective layer can combine the advantages of both inorganic and organic components to achieve superior battery performance. Hybrid protective layers can primarily be prepared using inorganic-organic/polymer combinations, MOF materials, COF materials, and MLD technology. While these methods have significantly improved the performance of sodium metal anodes, they each have their own challenges. For example, direct inorganic-organic/polymer mixing often results in poor interface contact, aggregation of inorganic particles within the organic matrix, and inadequate interface uniformity. More refined designs are needed to better integrate inorganic and organic components. MOF and COF materials, as protective layers, offer advantages such as tunable structures and strong design flexibility. However, they also have some drawbacks. MOFs generally have poor thermal stability and may not withstand high-temperature operations in practical working environments. COFs, on the other hand, suffer from low

mechanical strength and poor structural stability. MLD technology offers strong controllability, but its relatively complex fabrication process and high cost hinder widespread application. The design strategies and construction methods for inorganic-organic hybrid protective layers need further development to advance the practical application of sodium metal batteries.

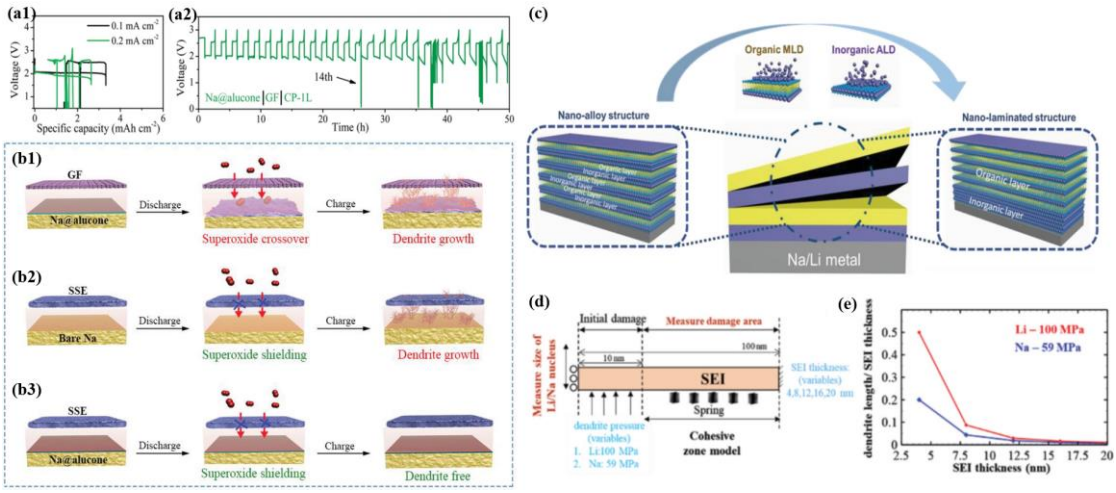

Figure 11. (**a**) Na-O_2 cells composed of GF separator and Na@alucone anode: (**a1**) discharge/charge profiles and (**a2**) cycling performance. (**b**) Schematic illustration of Na stripping/plating behaviors in Na-O_2 batteries with different configurations: (**b1**) Na@alucone anode with GF, (**b2**) bare Na anode with SSE, (**b3**) Na@alucone anode with SSE [108]. Reprinted with permission. Copyright 2021, Wiley-VCH (**c**) Schematic diagram of the fabrication of the nanoalloy and nano-laminated interfacial structures. (**d,e**) SEI delamination model based on mechanical analysis. (**d**) Schematic with initial and boundary conditions. (**e**) Plot of the SEI thicknesses against the resulting dendrite nucleation length [109]. Reprinted with permission. Copyright 2023, Wiley-VCH.

4. Summary and prospects

To clarify the protective effects of different types of artificial interface layers on sodium electrodes, Tables 1–3 summarize the electrochemical performance of various reported interface layers in recent years.

Table 1. Summary of the reported literature on inorganic interface engineering of sodium metal anodes.

Interphase	Technique	Na-cell	Capacity ($mAh \cdot cm^{-2}$) Current ($mA \cdot cm^{-2}$)	Life(h)	Ref.
NaF	Reacting with TREAT-HF	Na-Na	2,2	1000	[68]
NaF	Reacting with PTFE	Na-Na	1,1	1000	[69]
NaF, Na_xSn_y	Reacting with SnF_2	Na-Na	0.25,0.125	600	[70]

Table 1. *Cont.*

Interphase	Technique	Na-cell	Capacity ($mAh \cdot cm^{-2}$) Current ($mA \cdot cm^{-2}$)	Life(h)	Ref.
NaBr	Reacting with bromopropane	Na-Na Na-S	1,1	250 250	[71]
NaI	Treated with 2-iodopropane.	Na-Na Na-Cu	0.25,0.75 1,0.75	500 525	[72]
Na_3N, NaN_xO_y	Mechanical kneading approach	Na-Na	0.5,0.5	600	[73]
Na_3P	Red phosphorus (P) pretreatment	Na-Na	1,1	780	[74]
Na_3P, NaBr	Reaction between Na metal and PBr_3	Na-Na	1,1	750	[38]
$Na_{22}Ga_{39}$	Rolling the metal Ga on Na metal	Na-Na	6,1	468	[75]
Na-In	Reacting with metal chloride solution	Na-Na	2,2	790	[76]
Na_2Se, $Na_{15}Sn_4$	Reaction between SnSe and Na	Na-Na	0.5,1	2400	[77]
Al_2O_3	ALD	Na-Na	3,1	500	[26]
$NaAlO_x$	ALD	Na-Na	3,1	1300	[79]

Table 2. Summary of the reported literature on organic interface engineering of sodium metal anodes.

Interphase	Technique	Na-cell	Capacity ($mAh \cdot cm^{-2}$) Current ($mA \cdot cm^{-2}$)	Life(h)	Ref.
PhS_2Na_2	S_8reacts with para-dichlorobenzene (p-DB) and sodium	Na-Na	1,1	800	[81]
HCOONa, RONa	Spraying 1,3-dioxolane on Na metal	Na-Na	1,1	2500	[82]
HCOONa	By solid–gas reaction	Na-Na	2,1	2500	[83]
PVDF	PVDF sandwiched between GF and Na metal	Na-O_2	100 ($mA \cdot g^{-1}$) 100 ($mA \cdot g^{-1}$)	87	[85]
PVDF	Scalable doctor blade coating technique	Na-Na	1,1	1200	[86]

Table 3. Summary of the reported literature on inorganic-organic composite interface engineering of sodium metal anodes.

Interphase	Technique	Na-cell	Capacity ($mAh \cdot cm^{-2}$) Current ($mA \cdot cm^{-2}$)	Life(h)	Ref.
NaF, PVDF	By freestanding and implantable artificial protective layer	Na-Na	0.25,0.5	1200	[93]
Sn, PVDF	By doctor blade coating technology	Na-Na	1,1	2300	[91]
Bi, PVDF	By doctor blade coating technology	Na-Na	1,1	2700	[96]

Table 3. *Cont.*

Interphase	Technique	Na-cell	Capacity ($mAh \cdot cm^{-2}$) Current ($mA \cdot cm^{-2}$)	Life(h)	Ref.
NaF, KF, PTFE	Grinding $Na_{57}K$ with PTFE, then casting on current collector	Na-Na	0.5,0.5	1414	[97]
Sn, NaCl, PPO	Reacting with $SnCl_2$ and 4-chloro-2,6-dimethylphenol	Na-Na Na-O_2	4,4 0.5,0.5	2000 180	[98]
ZIF-62	Liqud MOF SSE	Na-Na	0.1,1	1000	[102]
sp^2 c-COF	COF separator	Na-Cu Na-Na	2,1 20,1	1000 1500	[103]
Alucone	MLD	Na-Na	1,1	270	[107]
Al_2O_3-Alucone	ALD, MLD	Na-Na	3,1	1500	[109]

Sodium metal, as an anode, has several advantages, including high theoretical energy density, low redox potential, abundant resources, and relatively low cost, making it an ideal material for next-generation energy storage. However, issues such as unavoidable dendrite growth, instability of the *in situ* SEI layer, and significant volume changes during cycling hinder its commercialization.

This paper first introduces the dendrite growth models for sodium metal anodes and the mechanisms of SEI layer evolution. It then categorizes the artificial SEI layers based on their composition characteristics (inorganic, organic, and inorganic-organic composites) and reviews the research progress in constructing artificial SEI layers. Although these research methods have significantly improved the stability of sodium metal anodes, there are still some issues that need to be addressed. For example, how can we further enhance the stability and mechanical strength of the SEI layer to cope with more complex real-world battery operating conditions? How can we more clearly explain the performance differences of various interface layers to provide a stronger theoretical basis for material selection? How can we reduce the cost of fabricating artificial SEI layers to enable large-scale production? These are the critical questions that need to be addressed. To this end, this paper proposes the following outlook:

(1) Optimizing the fabrication process of interface layers: Develop efficient and controllable fabrication processes for large-scale production. Research should focus on reducing the production costs of artificial interface layers, improving the consistency and reproducibility of the process, and shortening the fabrication time. With the continuous advancement of artificial intelligence and big data technologies, along with improvements in material fabrication equipment, we can leverage these innovations to optimize the fabrication processes and parameter settings for artificial SEI layers, achieving more precise and efficient interface control.

(2) Utilizing advanced characterization techniques: The nucleation process of sodium, the formation of SEI, and the mechanisms of dendrite growth remain unclear. Therefore, advanced characterization techniques are required to analyze these processes. For example, cryo-electron microscopy can effectively reduce electron beam damage to samples, preserving the integrity of the material's microstructure. *In-situ* XPS and FTIR can detect the

compositional evolution and structural changes of the SEI layer, while *in-situ* SEM and transmission electron microscopy (TEM) can monitor morphological changes during cycling in real time.

(3) Multi-scale modeling and prediction: Utilize multi-scale modeling techniques to conduct an in-depth analysis of artificial interface layers, predicting and optimizing their behavior from the atomic level to the macroscopic scale. By combining computer simulations, theoretical calculations, and experimental data, more accurate models of interface behavior can be developed, predicting the performance of interface layers under various operating conditions. For example, DFT calculations can be used to determine the surface energies of different components, allowing for the screening of more ideal artificial SEI coating materials. Finite element analysis (FEA) can be employed to simulate the electrochemical dynamics at the electrode/electrolyte interface, predicting the dendrite growth process. By fully utilizing these methods, trial-and-error costs can be reduced, and the research process can be accelerated.

(4) Combining artificial interface layers with anode-free/lean sodium metal anodes: Anode-free batteries are an emerging battery architecture that does not use active anode material; instead, alkali metal is directly electrochemically deposited onto the surface of the current collector. This approach can achieve higher cell voltage, lower costs, and greater energy density. However, most reports on artificial interface layers focus on thick Na foils, with limited research on constructing protective layers on anode-free structures or ultra-thin Na films. Therefore, deeper investigation into the feasibility of this approach is needed.

In conclusion, achieving high-performance, long-term stable sodium metal batteries is a challenging task. However, with continuous exploration and technological innovation by researchers, we believe that in the near future, protective strategies for sodium metal batteries will make revolutionary breakthroughs, becoming an indispensable part of next-generation energy storage materials.

Acknowledgments

This work did not receive any funding.

Conflicts of interest

The authors declare no conflicts of interest.

Authors' Contribution

Conceptualization and design: Xiaowei Zhu; methodology: Xiaowei Zhu, Wenwu Mo, Huanyu Li; software and validation: Xiaowei Zhu, Huanyu Li, Shaojie Hu; formal analysis: Xiaowei Zhu; investigation and data curation: Xiaowei Zhu, Wenwu Mo, Huanyu Li; resources: Xiaowei Zhu, Huanyu Li, Shaojie Hu; writing and original draft preparation: Xiaowei Zhu, Lijuan Zhang; writing, review and editing: Xiaowei Zhu, Lijuan Zhang;

supervision: Lijuan Zhang. All authors have read and agreed to the published version of the manuscript.

References

[1] Haines A, Smith KR, Anderson D, Epstein PR, McMichael AJ, *et al.* Policies for accelerating access to clean energy, improving health, advancing development, and mitigating climate change. *Lancet* 2007, 370(9594):1264–1281.

[2] Zhang B, Kang F, Tarascon JM, Kim JK. Recent advances in electrospun carbon nanofibers and their application in electrochemical energy storage. *Prog. Mater Sci.* 2016, 76:319–380.

[3] Matios E, Wang H, Wang C, Li W. Enabling Safe Sodium Metal Batteries by Solid Electrolyte Interphase Engineering: A Review. Ind. Eng. Chem. Res. 2019, 58 (23):9758–9780.

[4] Dunn B, Kamath H, Tarascon JM. Electrical Energy Storage for the Grid: A Battery of Choices. *Science* 2011, 334(6058):928–935.

[5] Liang Y, Zhao C, Yuan H, Chen Y, Zhang W, *et al.* A review of rechargeable batteries for portable electronic devices. *InfoMat.* 2019, 1(1):6–32.

[6] Henschel J, Horsthemke F, Stenzel YP, Evertz M, Girod S, *et al.* Lithium ion battery electrolyte degradation of field-tested electric vehicle battery cells - A comprehensive analytical study. *J. Power Sources* 2020, 447:277370.

[7] Gao R, Yang H, Wang C, Ye H, Cao F, *et al.* Fatigue-Resistant Interfacial Layer for Safe Lithium Metal Batteries. *Angew. Chem. Int. Ed.* 2021, 60 (48):25508–25513.

[8] Nam KH, Jeong S, Yu B, Choi JH, Jeon KJ, *et al.* Li-Compound Anodes: A Classification for High-Performance Li-Ion Battery Anodes. ACS NANO 2022, 16(9): 13704–13714.

[9] Hao H, Hutter T, Boyce BL, Watt J, Liu PC, *et al.* Review of Multifunctional Separators: Stabilizing the Cathode and the Anode for Alkali (Li, Na, and K) Metal-Sulfur and Selenium Batteries. *Chem. Rev.* 2022, 122 (9):8053–8125.

[10] Hwang JY, Myung ST, Sun YK. Recent Progress in Rechargeable Potassium Batteries. *Adv. Funct. Mater.* 2018, 28(43):1802938.

[11] Liu Y, Lu SW, Wang ZC, Xu JJ, Weng SX, *et al.* Weakly Polar Ether-Aided Ionic Liquid Electrolyte Enables High-Performance Sodium Metal Batteries over Wide Temperature Range. *Adv. Funct. Mater.* 2024, 34(28):2312295.

[12] Fan LL, Li XF. Recent advances in effective protection of sodium metal anode. *Nano Energy* 2018, 53: 630–642.

[13] Sun B, Li P, Zhang JQ, Wang D, Munroe P, *et al.* Dendrite-Free Sodium-Metal Anodes for High-Energy Sodium-Metal Batteries. *Adv. Mater.* 2018, 30(29):1801334.

[14] Wang P, Zhang G, Wei XY, Liu R, Gu JJ, *et al.* Bioselective Synthesis of a Porous Carbon Collector for High-Performance Sodium-Metal Anodes. *J. Am. Chem. Soc.* 2021, 143(9): 3280–3283.

[15] An Y, Fei H, Zeng G, Xu X, Ci L, *et al.* Vacuum distillation derived 3D porous current collector for stable lithium-metal batteries. *Nano Energy* 2018, 47:503–511.
[16] Lu X, Luo J, Matios E, Zhang Y, Wang H, *et al.* Enabling high-performance sodium metal anodes via A sodiophilic structure constructed by hierarchical Sb2MoO6 microspheres. *Nano Energy* 2020, 69:104446.
[17] Chen RC, Lu X, He QR, Yao ML, Yao TH, *et al.* Sb2S3 Nanorod Hierarchies Enabling Homogeneous Sodium Deposition for Dendrite-Free Sodium-Metal Batteries. *ACS Appl. Energy Mater.* 2022, 5(9):10952–10960.
[18] Seh ZW, Sun J, Sun Y, Cui Y. A Highly Reversible Room-Temperature Sodium Metal Anode. *ACS Cent. Sci.* 2015, 1(8):449–455.
[19] Zheng JM, Chen SR, Zhao WG, Song JH, Engelhard MH, *et al.* Extremely Stable Sodium Metal Batteries Enabled by Localized High-Concentration Electrolytes. *ACS Energy Lett.* 2018, 3(2):315–321.
[20] Wang LF, Ren NQ, Yao Y, Yang H, Jiang W. *et al.* Designing Solid Electrolyte Interfaces towards Homogeneous Na Deposition: Theoretical Guidelines for Electrolyte Additives and Superior High-Rate Cycling Stability. *Angew. Chem. Int. Ed.* 2023, 62(6):e202214372.
[21] Hou MJ, Zhou YJ, Liang F, Zhao HP, Ji DY, *et al.* Research progress of solid electrolyte interphase for sodium metal anodes. *Chem. Eng. J.* 2023, 475:146227.
[22] Zhao Q, Stalin S, Archer LA. Stabilizing metal battery anodes through the design of solid electrolyte interphases. *Joule* 2021, 5(5):1119–1142.
[23] Gan L, Wang K, Liu Y, Ahmad W, Wang X, *et al.* Dendrite-free Li-metal anode via a dual-function protective interphase layer for stable Li-metal pouch cell. *Sustainable Mater.Technol.* 2023, 36:e00585.
[24] Lee B, Paek E, Mitlin D, Lee SW. Sodium Metal Anodes: Emerging Solutions to Dendrite Growth. *Chem. Rev.* 2019, 119(8):5416–5460.
[25] Zhang Y, Ma L, Zhang L, Peng Z. Identifying a Stable Counter/Reference Electrode for the Study of Aprotic Na–O2Batteries. *J. Electrochem. Soc.* 2016, 163(7):A1270–A1274.
[26] Zhao Y, Goncharova LV, Lushington A, Sun Q, Yadegari H, *et al.* Superior Stable and Long Life Sodium Metal Anodes Achieved by Atomic Layer Deposition. *Adv. Mater.* 2017, 29(18):1606663.
[27] Chen X, Shen X, Li B, Peng HJ, Cheng XB, *et al.* Ion-Solvent Complexes Promote Gas Evolution from Electrolytes on a Sodium Metal Anode. *Angew. Chem. Int. Ed.* 2017, 57(3):734–737.
[28] Wang H, Yu D, Kuang C, Cheng L, Li W, *et al.* Alkali Metal Anodes for Rechargeable Batteries. *Chem* 2019, 5(2):313–338.
[29] Medenbach L, Bender CL, Haas R, Mogwitz B, Pompe C, *et al.* Origins of Dendrite Formation in Sodium-Oxygen Batteries and Possible Countermeasures. *Energy Technol.* 2017, 5(12):2265–2274.
[30] Cheng XB, Zhang R, Zhao CZ, Zhang Q. Toward Safe Lithium Metal Anode in Rechargeable Batteries: A Review. *Chem. Rev.* 2017, 117(15):10403–10473.

[31] Wang L, Zhou ZY, Yan X, Hou F, Wen L, *et al.* Engineering of lithium-metal anodes towards a safe and stable battery. *Energy Storage Mater.* 2018, 14:22–48.
[32] Chazalviel JN. Electrochemical aspects of the generation of ramified metallic electrodeposits. *Phys. Rev. A* 1990, 42(12):7355–7367.
[33] Rosso M, Brissot C, Teyssot A, Dollé M, Sannier L, *et al.* Dendrite short-circuit and fuse effect on Li/polymer/Li cells. *Electrochim. Acta* 2006, 51(25):5334–5340.
[34] Liu W, Liu P, Mitlin D. Tutorial review on structure-dendrite growth relations in metal battery anode supports. *Chem. Soc. Rev.* 2020, 49(20):7284–7300.
[35] Sand HJS III. On the concentration at the electrodes in a solution, with special reference to the liberation of hydrogen by electrolysis of a mixture of copper sulphate and sulphuric acid. *Lond. Edinb. Phil. Mag.* 1901, 1(1):45–79.
[36] Liu S, Gu B, Chen Z, Zhan R, Wang X, *et al.* Suppressing dendritic metallic Li formation on graphite anode under battery fast charging. *J. Energy Chem.* 2024, 91:484–500.
[37] Wang X, Lu J, Wu Y, Zheng W, Zhang H, *et al.* Building Stable Anodes for High-Rate Na-Metal Batteries. *Adv. Mater.* 2024, 36(16):2311256.
[38] Luo Z, Tao S, Tian Y, Xu L, Wang Y, *et al.* Robust artificial interlayer for columnar sodium metal anode. *Nano Energy* 2022, 97:107203.
[39] Shi SQ, Lu P, Liu ZY, Qi Y, Hector LG, *et al.* Direct Calculation of Li-Ion Transport in the Solid Electrolyte Interphase. *J. Am. Chem. Soc.* 2012, 134(37):15476–15487.
[40] Chen XR, Yao YX, Yan C, Zhang R, Cheng XB, *et al.* A Diffusion-Reaction Competition Mechanism to Tailor Lithium Deposition for Lithium-Metal Batteries. *Angew. Chem. Int. Ed.* 2020, 59(20):7743–7747.
[41] Hagopian A, Doublet ML, Filhol JS. Thermodynamic origin of dendrite growth in metal anode batteries. *Energy Environ. Sci.* 2020, 13 (12):5186–5197.
[42] Monroe C, Newman J. The impact of elastic deformation on deposition kinetics at lithium/polymer interfaces. *J. Electrochem. Soc.* 2005, 152(2):A396–A404.
[43] Lu X, Zhao HY, Qin YY, Matios E, Luo JM, *et al.* Building Fast Ion-Conducting Pathways on 3D Metallic Scaffolds for High-Performance Sodium Metal Anodes. *ACS nano* 2023, 17(11):10665–10676.
[44] Lu X, Chen RC, Shen SY, Li YY, Zhao HY, *et al.* Spatially Confined in Situ Formed Sodiophilic-Conductive Network for High-Performance Sodium Metal Batteries. *Nano Lett.* 2024, 24(18):5490–5497.
[45] Lee Y, Lee J, Lee J, Kim K, Cha A, *et al.* Fluoroethylene Carbonate-Based Electrolyte with 1 M Sodium Bis(fluorosulfonyl)imide Enables High-Performance Sodium Metal Electrodes. *ACS Appl. Mater. Interfaces* 2018, 10(17):15270–15280.
[46] Zhou WD, Li YT, Xin S, Goodenough JB. Rechargeable Sodium All-Solid-State Battery. *ACS Cent. Sci.* 2017, 3(1):52–57.
[47] Liang X, Pang Q, Kochetkov IR, Sempere MS, Huang H, *et al.* A facile surface chemistry route to a stabilized lithium metal anode. *Nat. Energy* 2017, 2(9):17119.
[48] Zhao Y, Adair KR, Sun XL. Recent developments and insights into the understanding of Na metal anodes for Na-metal batteries. *Energy Environ. Sci.* 2018, 11(10), 2673–2695.

[49] Hong YS, Li N, Chen H, Wang P, Song WL. In operando observation of chemical and mechanical stability of Li and Na dendrites under quasi-zero electrochemical field. *Energy Storage Mater.* 2018, 11:118–126.
[50] Peled E. The Electrochemical-Behavior of Alkali and Alkaline-Earth Metals in Non-Aqueous Battery Systems-The Solid Electrolyte Interphase Model. *J. Electrochem. Soc.* 1979, 126(12):2047–2051.
[51] Goodenough JB, Kim Y. Challenges for Rechargeable Li Batteries. *Chem. Mater* 2009, 22(3):587–603.
[52] Pirayesh P, Jin EZ, Wang YJ, Zhao Y. Na metal anodes for liquid and solid-state Na batteries. *Energy Environ. Sci.* 2024, 17(2):442–496.
[53] Lu X, Zhao XX, Ding SJ, Hu XF. 3D mixed ion/electron-conducting scaffolds for stable sodium metal anodes. *Nanoscale* 2024, 16(7):3379–3392.
[54] Ma LB, Cui J, Yao SS, Liu XM, Luo YS, *et al.* Dendrite-free lithium metal and sodium metal batteries. *Energy Storage Mater.* 2020, 27:522–554.
[55] Sun B, Xiong P, Maitra U, Langsdorf D, Yan K, *et al.* Design Strategies to Enable the Efficient Use of Sodium Metal Anodes in High-Energy Batteries. *Adv. Mater.* 2019, 32(18):1903891.
[56] Wei S, Xu S, Agrawral A, Choudhury S, Lu Y, *et al.* A stable room-temperature sodium-sulfur battery. *Nat. Commun.* 2016, 7(1):11722.
[57] Adelhelm P, Hartmann P, Bender CL, Busche M, Eufinger C, *et al.* From lithium to sodium: cell chemistry of room temperature sodium–air and sodium–sulfur batteries. *Beilstein J. Nanotechnol.* 2015, 6: 1016–1055.
[58] Yoshio M, Wang HY, Fukuda K, Hara Y, Adachi Y. Effect of carbon coating on electrochemical performance of treated natural graphite as lithium-ion battery anode material. *J. Electrochem. Soc.* 2000, 147(4): 1245–1250.
[59] Obrovac MN, Christensen L. Structural changes in silicon anodes during lithium insertion/extraction. *Electrochem. Solid-State Lett.* 2004, 7(5):A93–A96.
[60] Zhao Y, Yang XF, Kuo LY, Kaghazchi P, Sun Q, *et al.* High Capacity, Dendrite-Free Growth, and Minimum Volume Change Na Metal Anode. *Small* 2018, 14(20):1703717.
[61] Liu W, Liu P, Mitlin D. Review of Emerging Concepts in SEI Analysis and Artificial SEI Membranes for Lithium, Sodium, and Potassium Metal Battery Anodes. *Adv. Energy Mater.* 2020, 10(43): 2002297.
[62] Zhu L, Li Y, Zhao J, Liu J, Wang L, *et al.* Recent advanced development of stabilizing sodium metal anodes. *Green Energy Environ.* 2023, 8(5):1279–1307.
[63] Bao C, Wang B, Liu P, Wu H, Zhou Y, *et al.* Solid Electrolyte Interphases on Sodium Metal Anodes. *Adv. Funct. Mater.* 2020, 30(52):2004891.
[64] Wang T, Hua Y, Xu Z, Yu JS. Recent Advanced Development of Artificial Interphase Engineering for Stable Sodium Metal Anodes. *Small* 2021, 18(5): 2102250.
[65] He MF, Guo R, Hobold GM, Gao HN, Gallant BM. The intrinsic behavior of lithium fluoride in solid electrolyte interphases on lithium. *P. Natl. Acad. Sci. Usa.* 2020, 117(1):73–79.

[66] Xu J, Yang J, Qiu Y, Jin Y, Wang T, *et al.* Achieving high-performance sodium metal anodes: From structural design to reaction kinetic improvement. *Nano Res.* 2023, 17(3):1288–1312.
[67] Fan XL, Chen L, Ji X, Deng T, Hou SY, *et al.* Highly Fluorinated Interphases Enable High-Voltage Li-Metal Batteries. *Chem* 2018, 4(1):174–185.
[68] Cheng Y, Yang X, Li M, Li X, Lu X, *et al.* Enabling Ultrastable Alkali Metal Anodes by Artificial Solid Electrolyte Interphase Fluorination. *Nano Lett.* 2022, 22(11):4347–4353.
[69] Xu M, Li Y, Ihsan-Ul-Haq M, Mubarak N, Liu Z, *et al.* NaF-rich solid electrolyte interphase for dendrite-free sodium metal batteries. *Energy Storage Mater.* 2022, 44:477–486.
[70] Damircheli R, Hoang B, Castagna Ferrari V, Lin CF. Fluorinated Artificial Solid–Electrolyte–Interphase Layer for Long-Life Sodium Metal Batteries. *ACS Appl. Mater. Interfaces* 2023, 15(47):54915–54922.
[71] Choudhury S, Wei S, Ozhabes Y, Gunceler D, Zachman MJ, *et al.* Designing solid-liquid interphases for sodium batteries. *Nat. Commun.* 2017, 8(1): 898.
[72] Tian H, Shao H, Chen Y, Fang X, Xiong P, *et al.* Ultra-stable sodium metal-iodine batteries enabled by an in-situ solid electrolyte interphase. *Nano Energy* 2019, 57:692–702.
[73] Wang X, Fu L, Zhan R, Wang L, Li G, *et al.* Addressing the Low Solubility of a Solid Electrolyte Interphase Stabilizer in an Electrolyte by Composite Battery Anode Design. *ACS Appl. Mater. Interfaces* 2021, 13(11): 13354–13361.
[74] Shi P, Zhang S, Lu G, Wang L, Jiang Y, *et al.* Red Phosphorous-Derived Protective Layers with High Ionic Conductivity and Mechanical Strength on Dendrite-Free Sodium and Potassium Metal Anodes. *Adv. Energy Mater.* 2020, 11(5):2003381.
[75] Lv X, Tang F, Yao Y, Xu C, Chen D, *et al.* Sodium–gallium alloy layer for fast and reversible sodium deposition. *SusMat.* 2022, 2(6):699–707.
[76] Moorthy M, Moorthy B, Ganesan BK, Saha A, Yu S, *et al.* A Series of Hybrid Multifunctional Interfaces as Artificial SEI Layer for Realizing Dendrite Free, and Long-Life Sodium Metal Anodes. *Adv. Funct. Mater.* 2023, 33(42):2300135.
[77] Cao L, Guo J, Feng Y, Li Y, Qiu Y, *et al.* A Rooted Multifunctional Heterogeneous Interphase Layer Enabled by Surface-Reconstruction for Highly Durable Sodium Metal Anodes. *Adv. Funct. Mater.* 2024, 34(18):2313962.
[78] Mäntymäki M, Ritala M, Leskelä M. Metal Fluorides as Lithium-Ion Battery Materials: An Atomic Layer Deposition Perspective. *Coatings* 2018, 8(8):277.
[79] Jin E, Tantratian K, Zhao C, Codirenzi A, Goncharova LV, *et al.* Ionic Conductive and Highly-Stable Interface for Alkali Metal Anodes. *Small* 2022, 18(33):2203045.
[80] Shi P, Wang X, Cheng X, Jiang Y. Progress on Designing Artificial Solid Electrolyte Interphases for Dendrite-Free Sodium Metal Anodes. *Batteries* 2023, 9(7):345.
[81] Zhu M, Wang G, Liu X, Guo B, Xu G, *et al.* Dendrite-Free Sodium Metal Anodes Enabled by a Sodium Benzenedithiolate-Rich Protection Layer. *Angew. Chem. Int. Ed.* 2020, 59(16):6596–6600.

[82] Lu Q, Omar A, Ding L, Oswald S, Hantusch M, *et al.* A facile method to stabilize sodium metal anodes towards high-performance sodium batteries. *J. Mater. Chem. A* 2021, 9(14):9038–9047.

[83] Wang C, Zheng Y, Chen ZN, Zhang R, He W, *et al.* Robust Anode-Free Sodium Metal Batteries Enabled by Artificial Sodium Formate Interface. *Adv. Energy Mater.* 2023, 13(22): 2204125.

[84] Tamwattana O, Park H, Kim J, Hwang I, Yoon G, *et al.* High-Dielectric Polymer Coating for Uniform Lithium Deposition in Anode-Free Lithium Batteries. *ACS Energy Lett.* 2021, 6(12), 4416–4425.

[85] Ma JL, Yin YB, Liu T, Zhang XB, Yan JM, *et al.* Suppressing Sodium Dendrites by Multifunctional Polyvinylidene Fluoride (PVDF) Interlayers with Nonthrough Pores and High Flux/Affinity of Sodium Ions toward Long Cycle Life Sodium Oxygen-Batteries. *Adv. Funct. Mater.* 2018, 28(13):1703931.

[86] Hou Z, Wang W, Yu Y, Zhao X, Chen Q. Poly (vinylidene difluoride) coating on Cu current collector for high-performance Na metal anode. *Energy Storage Mater.* 2020, 24:588–593.

[87] Meyerson ML, Papa PE, Heller A, Mullins CB. Recent Developments in Dendrite-Free Lithium-Metal Deposition through Tailoring of Micro- and Nanoscale Artificial Coatings. *ACS Nano* 2020, 15(1):29–46.

[88] Bae J, Qian Y, Li Y, Zhou X, Goodenough JB, Yu G. Polar polymer–solvent interaction derived favorable interphase for stable lithium metal batteries. *Energy Environ. Sci.* 2019, 12(11):3319–3327.

[89] Xiao J, Zhai P, Wei Y, Zhang X, Yang W, *et al.* In-Situ Formed Protecting Layer from Organic/Inorganic Concrete for Dendrite-Free Lithium Metal Anodes. *Nano Lett.* 2020, 20(5):3911–3917.

[90] Li S, Fan L, Lu Y. Rational design of robust-flexible protective layer for safe lithium metal battery. *Energy Storage Mater.* 2019, 18:205–212.

[91] Chen Q, Hou Z, Sun Z, Pu Y, Jiang Y, *et al.* Polymer–Inorganic Composite Protective Layer for Stable Na Metal Anodes. *ACS Appl. Energy Mater.* 2020, 3(3):2900–2906.

[92] Kang Q, Li Y, Zhuang Z, Wang D, Zhi C, *et al.* Dielectric polymer based electrolytes for high-performance all-solid-state lithium metal batteries. *J. Energy Chem.* 2022, 69:194–204.

[93] Wang S, Jie Y, Sun Z, Cai W, Chen Y. An Implantable Artificial Protective Layer Enables Stable Sodium Metal Anodes. *ACS Appl. Energy Mater.* 2020, 3(9):8688–8694.

[94] Deng X, Chawla N, Chawla KK, Koopman M. Deformation behavior of (Cu, Ag)–Sn intermetallics by nanoindentation. *Acta Mater.* 2004, 52(14):4291–4303.

[95] Wang G, Yu F, Zhang Y, Zhang Y, Zhu M, *et al.* 2D Sn/C freestanding frameworks as a robust nucleation layer for highly stable sodium metal anodes with a high utilization. *Nano Energy* 2021, 79: 105457.

[96] Zhang J, Wang S, Wang W, Li B. Stabilizing sodium metal anode through facile construction of organic-metal interface. *J. Energy Chem.* 2022, 66:133–139.

[97] Tai Z, Liu Y, Yu Z, Lu Z, Bondarchuk O, *et al.* Non-collapsing 3D solid-electrolyte interphase for high-rate rechargeable sodium metal batteries. *Nano Energy* 2022, 94:106947.

[98] Liu P, Miao L, Sun Z, Chen X, Si Y, *et al.* Inorganic–Organic Hybrid Multifunctional Solid Electrolyte Interphase Layers for Dendrite-Free Sodium Metal Anodes. *Angew. Chem. Int. Ed.* 2023, 62(47):e202312413.

[99] Xu J, Xu Y, Lai C, Xia T, Zhang B, *et al.* Challenges and perspectives of covalent organic frameworks for advanced alkali-metal ion batteries. *Sci. China Chem.* 2021, 64(8):1267–1282.

[100]Wang J, Yue X, Xie Z, Abudula A, Guan G. MOFs-derived transition metal sulfide composites for advanced sodium ion batteries. *Energy Storage Mater.* 2021, 41:404–426.

[101]Qian J, Li Y, Zhang M, Luo R, Wang F, *et al.* Protecting lithium/sodium metal anode with metal-organic framework based compact and robust shield. *Nano Energy* 2019, 60:866–874.

[102]Miao X, Wang P, Sun R, Li J, Wang Z, *et al.* Liquid Metal-Organic Frameworks In-Situ Derived Interlayer for High-Performance Solid-State Na-Metal Batteries. *Adv. Energy Mater.* 2021, 11(47): 2102396.

[103]Kang T, Sun C, Li Y, Song T, Guan Z, *et al.* Dendrite-Free Sodium Metal Anodes Via Solid Electrolyte Interphase Engineering with a Covalent Organic Framework Separator. *Adv. Energy Mater.* 2023, 13(15): 2204083.

[104]Zhao Y, Zheng K, Sun X. Addressing Interfacial Issues in Liquid-Based and Solid-State Batteries by Atomic and Molecular Layer Deposition. *Joule* 2018, 2(12):2583–2604.

[105]Sullivan M, Tang P, Meng X. Atomic and Molecular Layer Deposition as Surface Engineering Techniques for Emerging Alkali Metal Rechargeable Batteries. *Molecules* 2022, 27(19):6170.

[106]Sun Y, Zhao Y, Wang J, Liang J, Wang C, *et al.* A Novel Organic “Polyurea” Thin Film for Ultralong-Life Lithium-Metal Anodes via Molecular-Layer Deposition. *Adv. Mater.* 2018, 31(4):1806541.

[107]Zhao Y, Goncharova LV, Zhang Q, Kaghazchi P, Sun Q, *et al.* Inorganic–Organic Coating via Molecular Layer Deposition Enables Long Life Sodium Metal Anode. *Nano Lett.* 2017, 17(9):5653–5659.

[108]Lin X, Sun Y, Sun Q, Luo J, Zhao Y, *et al.* Reviving Anode Protection Layer in Na-O2 Batteries: Failure Mechanism and Resolving Strategy. *Adv. Energy Mater.* 2021, 11(11):2003789.

[109]Pirayesh P, Tantratian K, Amirmaleki M, Yang F, Jin E, *et al.* From Nanoalloy to Nano-Laminated Interfaces for Highly Stable Alkali-Metal Anodes. *Adv. Mater.* 2023, 35(29):2301414.